WIND-TUNNEL RESEARCH ON THE MECHANICS OF
PLUMES IN THE ATMOSPHERIC SURFACE LAYER

PART II

by

M. Poreh[1] and J. E. Cermak[2]

WIND-TUNNEL SIMULATION OF DIFFUSION IN AN
ATMOSPHERIC SURFACE LAYER WITH AN
ELEVATED INVERSION

-ANNUAL REPORT-

prepared for

The views, opinions, and/or findings contained in this report are those
of the author(s) and should not be construed as an official Department
of the Army position, policy, or decision, unless so designated by other
documentation.

May 1985

CER84-85MP-JEC47
Project No. 5-32512

[1]David T. Siegel Professor of Hydraulics, Technion, Haifa, Israel,
 Colorado State University Wind Engineering Scholar for 1984-85.
[2]Professor, Fluid Mechanics and Wind Engineering Program, Colorado State
 University.

REPORT DOCUMENTATION PAGE

1a. REPORT SECURITY CLASSIFICATION	1b RESTRICTIVE MARKINGS
Unclassified	

2a. SECURITY CLASSIFICATION AUTHORITY	3 DISTRIBUTION / AVAILABILITY OF REPORT
2b. DECLASSIFICATION / DOWNGRADING SCHEDULE NA	

4. PERFORMING ORGANIZATION REPORT NUMBER(S)	5. MONITORING ORGANIZATION REPORT NUMBER(S)

6a. NAME OF PERFORMING ORGANIZATION	6b. OFFICE SYMBOL (If applicable)	7a. NAME OF MONITORING ORGANIZATION
Fluid Dynamics and Diffusion Laboratory		CDR/DIR

6c. ADDRESS (City, State, and ZIP Code)	7b. ADDRESS (City, State, and ZIP Code)
Department of Civil Engineering Colorado State University Fort Collins, Colorado 80523	Chemical Systems Laboratory Attn: DRDAR-CLB-PS (Dr. E. Stuebing) Aberdeen Proving Ground, Maryland 21010

8a. NAME OF FUNDING/SPONSORING ORGANIZATION	8b. OFFICE SYMBOL (If applicable)	9. PROCUREMENT INSTRUMENT IDENTIFICATION NUMBER

8c. ADDRESS (City, State, and ZIP Code)	10. SOURCE OF FUNDING NUMBERS			
	PROGRAM ELEMENT NO.	PROJECT NO.	TASK NO.	WORK UNIT ACCESSION NO.

11. TITLE (Include Security Classification)
Wind-Tunnel Research on the Mechanics of Plumes in the Atmospheric Surface Layer, Part II: Wind-Tunnel Simulation of Diffusion in an Atmospheric Surface Layer with an Elevated Inversio

12. PERSONAL AUTHOR(S)
M. Poreh and J. E. Cermak

13a. TYPE OF REPORT Annual Progress Report	13b. TIME COVERED FROM ___ TO ___	14. DATE OF REPORT (Year, Month, Day) 1985, May	15. PAGE COUNT

16. SUPPLEMENTARY NOTATION
This study was sponsored by the Army Smoke Research Program, Chemical Systems Laboratory, Aberdeen Proving Ground, Maryland

17. COSATI CODES			18. SUBJECT TERMS (Continue on reverse if necessary and identify by block number)
FIELD	GROUP	SUB-GROUP	

19. ABSTRACT (Continue on reverse if necessary and identify by block number)

Diffusion of neutrally buoyant plumes emitted at various heights within a convective boundary layer capped by an inversion was simulated in a meteorological wind tunnel. Measurements were made of mean and fluctuating velocities and temperatures and of the diffusing plumes. When presented in a dimensionless coordinate system based on the buoyant heat flux and the thickness of the convective layer, the data appear to be consistent with available data from field studies and water-tank simulations and exhibit a unique pattern of diffusion which is related to the nature of the thermals and the downdrafts within the convective boundary layer.

20. DISTRIBUTION/AVAILABILITY OF ABSTRACT ☐ UNCLASSIFIED/UNLIMITED ☐ SAME AS RPT. ☐ DTIC USERS	21. ABSTRACT SECURITY CLASSIFICATION
22a. NAME OF RESPONSIBLE INDIVIDUAL	22b. TELEPHONE (Include Area Code)	22c. OFFICE SYMBOL

DD FORM 1473, 84 MAR   83 APR edition may be used until exhausted.   SECURITY CLASSIFICATION OF THIS PAGE
All other editions are obsolete.

ABSTRACT

Diffusion of neutrally buoyant plumes emitted at various heights within a convective boundary layer capped by an inversion was simulated in a meteorological wind tunnel. Measurements were made of mean and fluctuating velocities and temperatures and of the diffusing plumes. When presented in a dimensionless coordinate system based on the buoyant heat flux and the thickness of the convective layer, the data appear to be consistent with available data from field studies and water-tank simulations and exhibit a unique pattern of diffusion which is related to the nature of the thermals and the downdrafts within the convective boundary layer.

KEY WORDS

3

CONTENTS

LIST OF FIGURES

WIND-TUNNEL RESEARCH ON THE MECHANICS OF
PLUMES IN THE ATMOSPHERIC SURFACE LAYER

1   INTRODUCTION

The early morning atmospheric surface layer (ASL), particularly after clear nights with weak winds, is usually stably stratified. As the sun rises and heats the ground, a positive heat flux from the ground to the ASL is established, which heats and changes the nature of the lower layer, up to a height h(t). The height h(t), which increases with time, identifies the base of the inversion. A typical example of potential temperature profiles at different times of the day, in such instances, is shown in Figure 1.

The turbulence below the inversion is due to both mechanical, shear-generated turbulence, which decreases rapidly with the distance from the ground, and convective turbulence generated by the upward convection of heat. The convective turbulence increases with height and thus, when wind speed is weak, it dominates the character of the ASL. The boundary layer flow below the inversion is termed the Convective Boundary Layer (CBL).

The CBL is usually idealized as composed of several layers with distinct properties (Caughey, 1981)[4]. The layer near the ground, where the wind shear is the primary cause for turbulence, is called the surface layer. The convective turbulent velocity created by a heat flux $\rho C_p \overline{w'\theta'}_o$, is characterized by a velocity scale

$$w_1 = (z \; g \; \overline{w'\theta'}_o / \theta)^{1/3} \tag{1}$$

whereas the velocity scale of the mechanical turbulence is given by the shear velocity v^*. Thus, the ratio of convective to mechanical turbulence, which is proportioned to $\overline{w_1/v^*}$ can be expressed by the dimensionless ratio

$$-\frac{z}{L} = \left[\frac{kz \; g \; \overline{w'\theta'}_o}{(v^*)^3 \; \theta} \right]^{1/3} \tag{2}$$

where

$$L = -\left[(v^*)^3 \theta / (kg \; \overline{w'\theta'}_o) \right]^{1/3} \tag{3}$$

is the Monin-Obukhov length, and $k = 0.4$.

The thickness of the surface layer is of the order of L. Very close to the ground, where $-z/L$ is small, mechanical turbulence is dominant. When $-z/L$ is of the order of 1 or larger, the relative contribution of mechanical shear is drastically reduced.
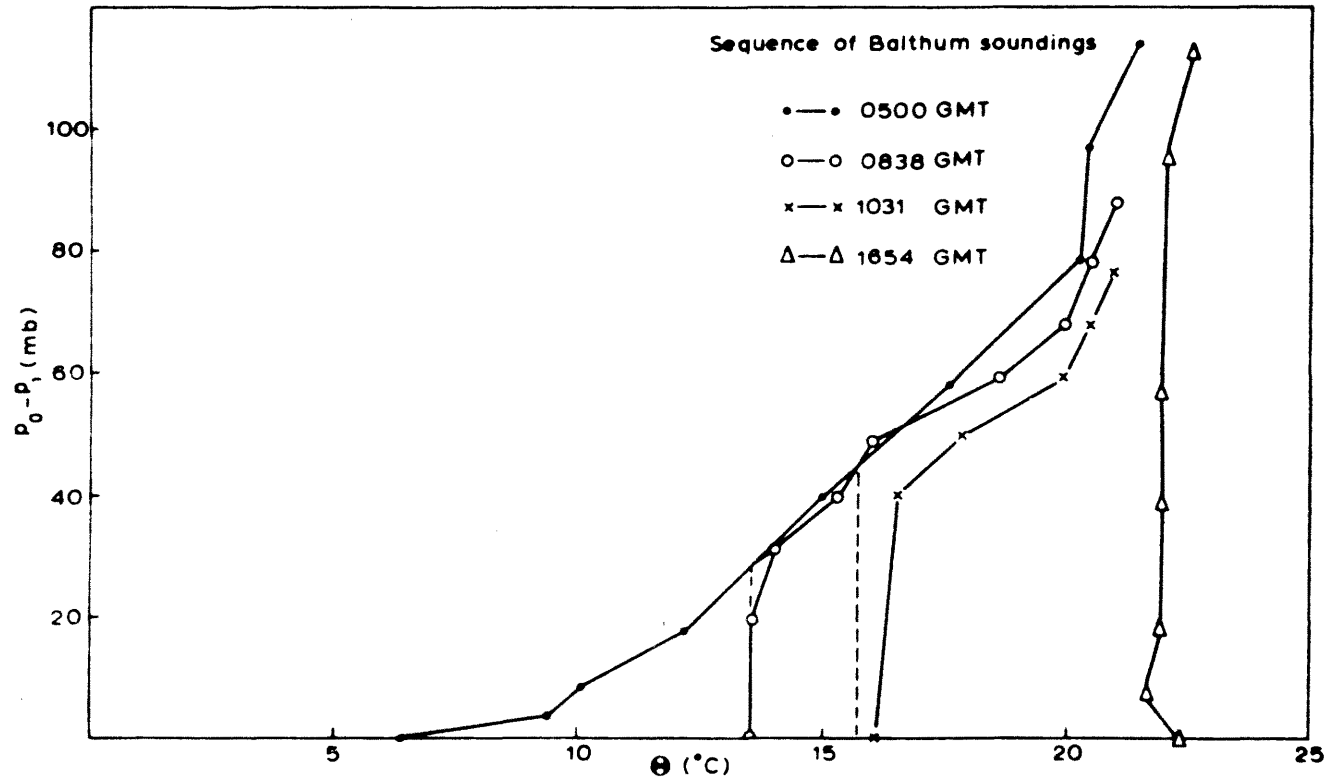
Figure 1. Potential temperature profiles showing the increase in the inversion height during the day. The height is given by the pressure difference (Chorley et al., 1975)[6].

The free convection layer is the layer above the surface layer, where the shear velocity is no longer important and the flow characteristics are determined by the height z and the heat flux. Observations suggest that the height of the free convection layer is of the order of 0.1 h. Thus, for a free convection layer to exist it is necessary that $h/L > 10$.

The mixed layer is the region above the free convection layer, where the structure of turbulence is independent of both v^* and z. The controlling parameters in this layer are the heat flux and the height of the inversion base h. The velocity scale in the layer is thus

$$w^* = (hg \; \overline{w'\theta'}_o \; /\theta)^{1/3} \tag{4}$$

and the temperature scale is

$$T^* = \frac{\overline{w'\theta'}_o}{w^*} . \tag{5}$$

The layer close to the inversion base is called the entrainment interfacial layer. Here, turbulence structure is determined by the entrainment process, and the exact characteristics of the layer are affected by the strength of the stable stratification of the flow above it. It roughly extends from 0.8h to 1.2h. This observation indicates that one should not expect to find a very localized sharp decrease of turbulence at h, but rather a gradual decay of turbulence with height. Indeed, Figure 2, from Caughey (1981)[4], clearly shows that σ_w/w^*, which is maximum in the mixed layer, decreases gradually with height around h, and at z/h = 1.1 it is reduced from its maximum value, at the center of the mixed layer, by only a factor of three. Clearly, one cannot expect the base of the inversion, in much cases, to act as a lid which reflects the diffusing contaminants from a well defined height.

The above multilayer idealization of the CBL applies best when $h/|L| >> 10$. When $h/|L|$ is of the order of 10, the structure of the CBL is still dominated by the convective turbulence, as $w^* > v^*$, however, mechanical turbulence cannot be completely ignored (Caughey, 1981)[4].

The characteristics of the CBL have been observed in a few extensive field experiments, such as the Minnesota experiment (Isumi and Caughey, 1976)[11] and the Ashchurch experiment (Caughey and Palmer, 1979)[3]. Numerical models have also been used to simulate the features of this layer (Deardorff, 1970, 1972, 1974[7-9]; and Lamb, 1978, 1981)[12,14] but perhaps the most dramatic simulation of the CBL and particularly of diffusion within the CBL has been made in the famous water-tank experiments of Willis and Deardorff (1974, 1976, 1978, 1979, 1983)[17-21]. In these experiments a stagnant stably stratified body of water was heated
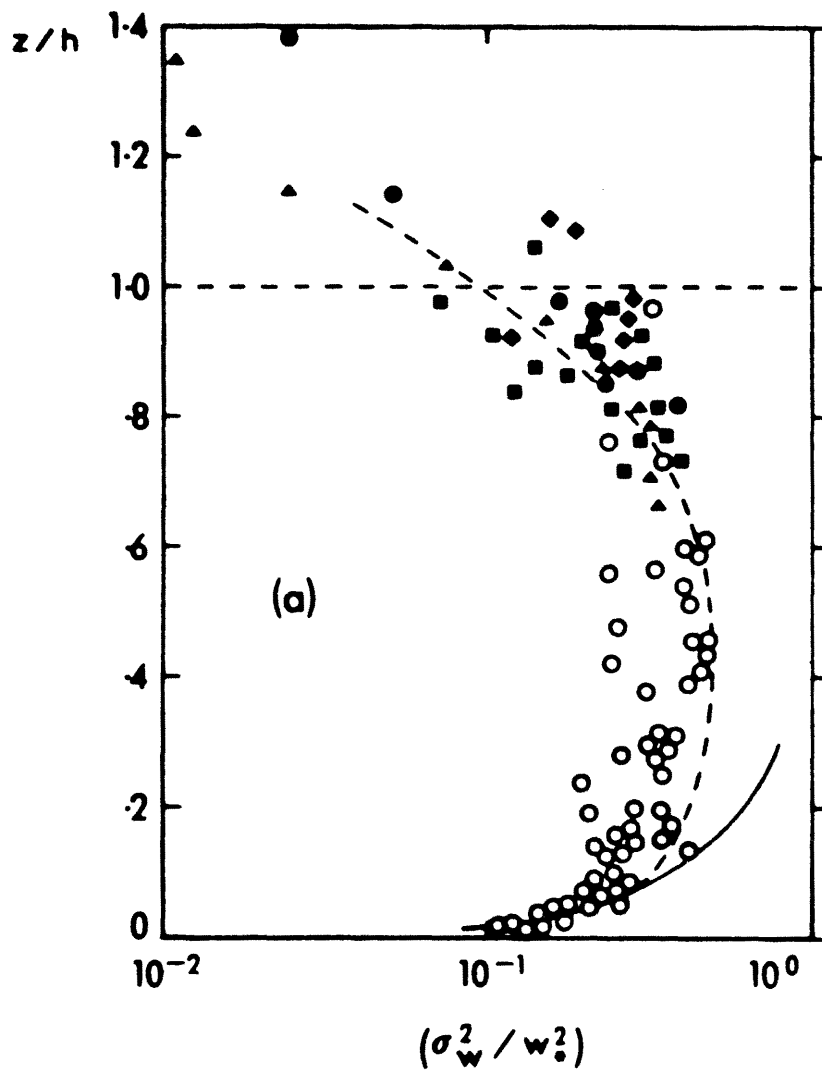
Figure 2. Normalized vertical variance (from Caughey and Palmer, 1979)[3].

from below. A mixed layer was formed, up to a height h(t) above the floor of the tank, and the characteristics of turbulence and of the diffusion within this layer were observed and recorded. The mean velocity U of the flow in these experiments was zero and so was the value of the shear. Thus, water tank simulations cannot produce the effect of shear generated turbulence, which might be influential for values of $h/|L|$ smaller than, or of the order of one.

Since the results obtained in the water-tank simulations of diffusion within the CBL have been rather surprising, and in a way contrary to those obtained by both Gaussian prediction models and gradient type diffusion models, it is of particular interest to test the results in the real atmosphere as well as to simulate diffusion in CBL, particularly at the lower range of $h/|L|$, without neglecting the possible effect of the shear.

In 1982 and 1983 diffusion experiments within a CBL were carried out at the Boulder Atmospheric Observatory (BAO). Preliminary results from these experiments were published by Briggs (1984a)[1]. In 1983 the authors studied the diffusion of neutrally buoyant plumes in a simulated CBL created in the Meteorological Wind Tunnel (MWT) at Colorado State University (Poreh and Cermak, 1984)[16]. The diffusion pattern was measured up to a dimensional distance of $x^* = xw^*/(hU) = O(1)$ from the source and was found to be similar to that measured in the water-tank simulation for equivalent values of $t^* = tw^*/h$.

It was recognized, however, that the experimental set up used in these wind-tunnel simulations had two shortcomings. The dimensionless distance of the source from the leading edge of the hot section of the MWT floor was approximately $x^* = 1.2$. It has been estimated (Briggs, 1984b)[2] that a distance of $x^* = 2$ is required for a full development of the large convective eddies. Thus, it is quite possible that the structure of the upper part of the CBL was not fully simulated in these experiments. Moreover, the temperature gradient in the stably stratified layer above h was rather mild and it is possible that the inversion height was not correctly estimated. Apparently, these shortcomings have not affected the similarity between the wind tunnel and the water-tank simulations, since the measurements were limited to diffusion from relatively low-level sources at $z^s/h < 0.33$ and to values of $x^* < 1.1$. During the time $t^* = 1.1$ the plumes, which initially descend to the ground, are primarily affected by the lower portion of the CBL, which was appropriately simulated.

For this reason it was decided to change the experimental configuration in the MWT in order to achieve a stronger inversion above h and to measure the pattern of diffusing plumes from sources at different heights.

11

2   EXPERIMENTAL APPARATUS AND PROCEDURES

The experiments were conducted in the MWT in the Fluid Dynamics and Diffusion Laboratory at Colorado State University. The design and operation of the 2m x 2m x 27m MWT are described in detail by Cermak (1981)[5].

Eleven brine-cooled aluminum plates were placed across the test section at three locations of the upwind section of the MWT between two Masonite plates, as described schematically in Figure 3. A photograph of the plates is shown in Figure 4.

The air entered the wind tunnel at a speed of approximately 1 m/sec and a temperature of approximately 58°C. The air layer passing in the space between the two Masonite plates was cooled by the aluminum plates, whose surface temperature was maintained at approximately 0°C, due to the formation of a thin layer of ice on the plates. Eight small fans were placed in this space to insure lateral homogeneity. The air then passed through a honeycomb and a screen to reduce turbulence.

The leading edge of the hot wind-tunnel floor was located at a distance of 2.2 m from the screen. Since the lowest, 15 cm thick air layer was relatively hot, intensive mixing started even before the air reached the hot floor. The surface temperature of the 12 m long hot-section of the floor was maintained at approximately 110°C. The heat flux from the floor was estimated to be approximately 0.3°C-m/s.

Velocities were measured with a constant-temperature, cross-film, anemometer sensor, type TSI 1241-10, with a resistance-wire temperature sensor mounted at close proximity. The sensors were calibrated in a temperature and velocity controlled calibrator. An empirical equation relating anemometer voltage, velocity and temperature was developed and incorporated into the on-line computer data collection system, permitting instantaneous readings of the velocities and temperature.

Unfortunately, the very large velocity and temperature fluctuations increased the inherent errors of the hot-film system and thus one should regard the presented turbulent data only as very rough estimates.

A neutrally buoyant hydrocarbon tracer was released from horizontal 0.63 cm glass tube located at z^s = 0.7, 10, and 24.5 cm above the floor at a distance of 3.60 m from the leading edge of the hot floor. The position of the source is designated in this report as x = 0. The average horizontal exit velocity of the tracer gas was 0.7 m/sec, in most of the experiments. During the measurements of the diffusion plume at x = 3.7 and 5.4 m, the exit velocity and discharge of the tracer was doubled and quadrupled to increase the concentration at these distances. The temperature of the exit tracer gas was maintained at the average temperature at z^s by passing the gas through a 90 cm long, horizontal, thin-walled brass tube at the source height.
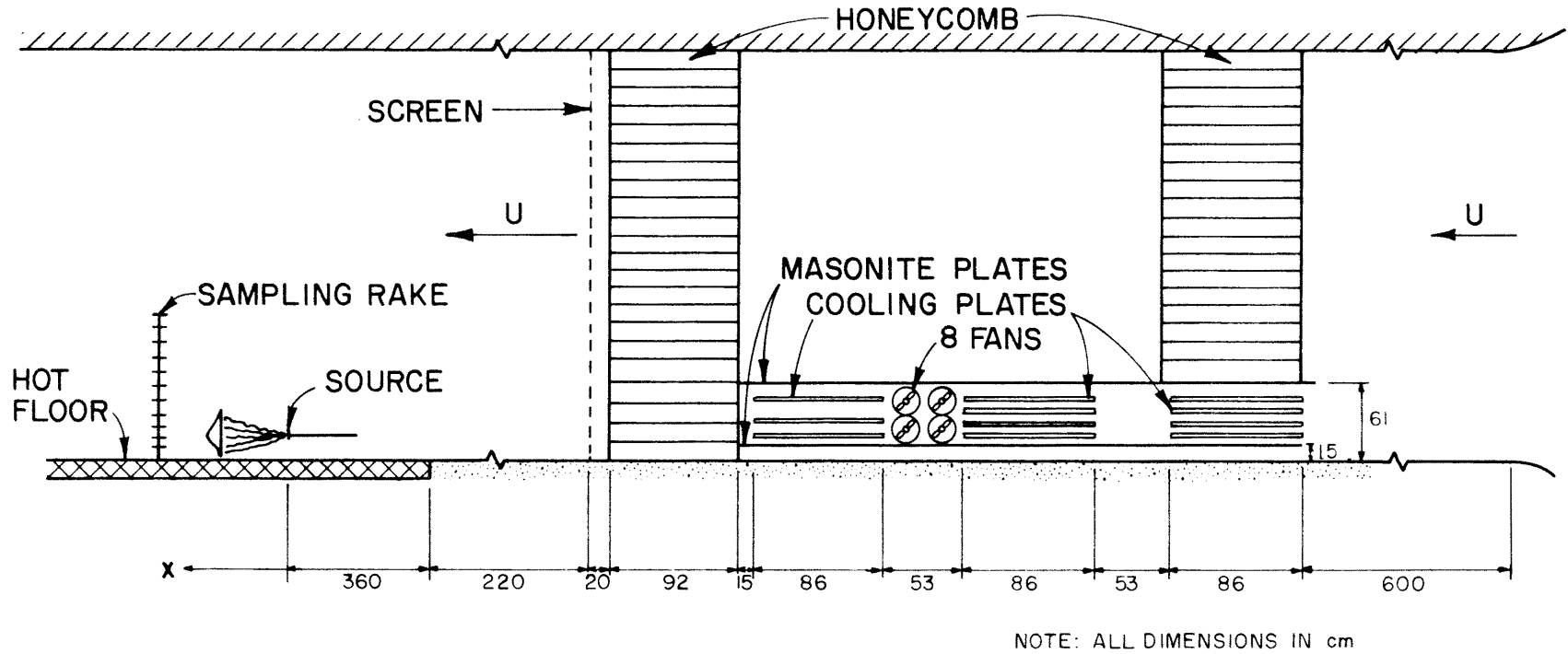
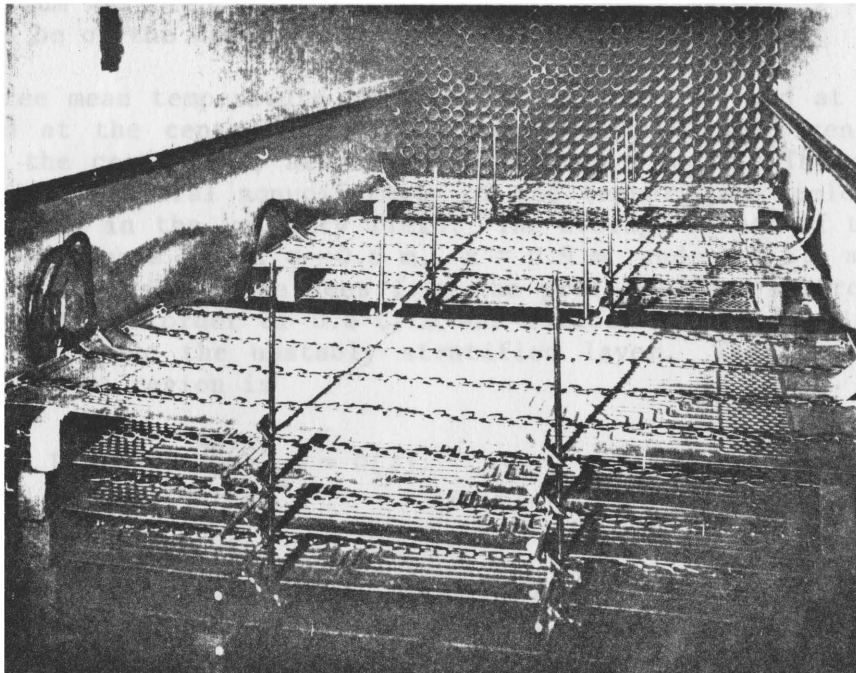Figure 3. Schematic description of the wind-tunnel configuration.

Figure 4. Photograph of the cooling plates in the upwind part of the wind tunnel (upper Masonite plate and honeycomb removed).

3   THE EXPERIMENTAL RESULTS

3.1   The Velocity and Temperature Measurements

The mean horizontal velocity profiles measured at $x = -0.6$ m, $x = 0.9$ m and $x = 5.4$ m are shown in Figure 5. Only a slight horizontal inhomogeneity between the first two stations is observed and it appears that in the region where the diffusion experiments took place, the mean horizontal velocity in the region 0.1 m $< z < 0.5$ m was almost constant and close to $U = 1.0$ m/s. This value will be assumed to be the representative mean horizontal velocity of the simulated CBL. The velocity above $z = 0.4$ m appears to decrease slightly with height. The maximum measured velocity gradient at approximately $z = 0.5$ m, was found to be of the order of 1.0 (m/s)/m.

Three mean temperature profiles at $x = 0.9$ m and at $x = 5.4$ m, measured at the centerline of the tunnel and 40 cm of center on each side of the centerline, are shown in Figures 6 and 7. The measurements show a small lateral nonuniformity of the temperature field, which was not observed in the velocity field. The average values of the temperature measurements at $x = -0.6$ m, $x = 0.9$ m and $x = 5.4$ m are shown in Figures 8 and 9. One sees from the profiles that a strong positive gradient of the order of $0.6°C/cm$ was established at $x = -0.6$ m and $x = 0.9$ m above the unstably stratified layer. The local Richardson number at that region is

$$R_i = \frac{g}{\theta} \frac{\partial\theta/\partial z}{(\partial u/\partial z)^2} = 0(2).$$

Apparently, this local value of R_i is not sufficient to prevent a rather rapid erosion of the stable layer, as evident from the temperature profile at $x = 5.4$ m, possibly because the thickness of the stable layer was not large enough.

There is no agreed upon method to determine the thickness of the CBL, $h(x)$, developed in such experiments. The minimum of the average temperature profile (T_{min}) appears to be at $z = 30$ cm above the floor, however, the positive temperature gradient below $z = 40$ cm is rather mild and could not produce an effective lid over the lower mixed layer. Using the log-linear plot of the temperature profile, shown in Figure 9, it was arbitrarily decided to define $h(x)$ by the intersection of the line $T = a \log z$, describing the profile at the region of maximum positive temperature gradient at each station, with the line $T = T_{min}$, as shown in Figure 9 for $x = -0.6$. Using this algorithm, values of $h(-0.6) = 0.35$ m, $h(0.9) = 0.37$ m and $h(5.4) = 0.42$ m were obtained. Thus, an average value of $h = 0.40$ m, for the region $0 < x < 5.4$ m, where the diffusion experiments took place, was chosen.

The heat flux from the floor in this region was estimated from the balance of the heat flux values at $x = 0.9$ m and $x = 5.4$ m. This estimate gave a value of $\overline{w'\theta'}_o = 0.3°C$ m/s. Using Eqs. (4) and (5)
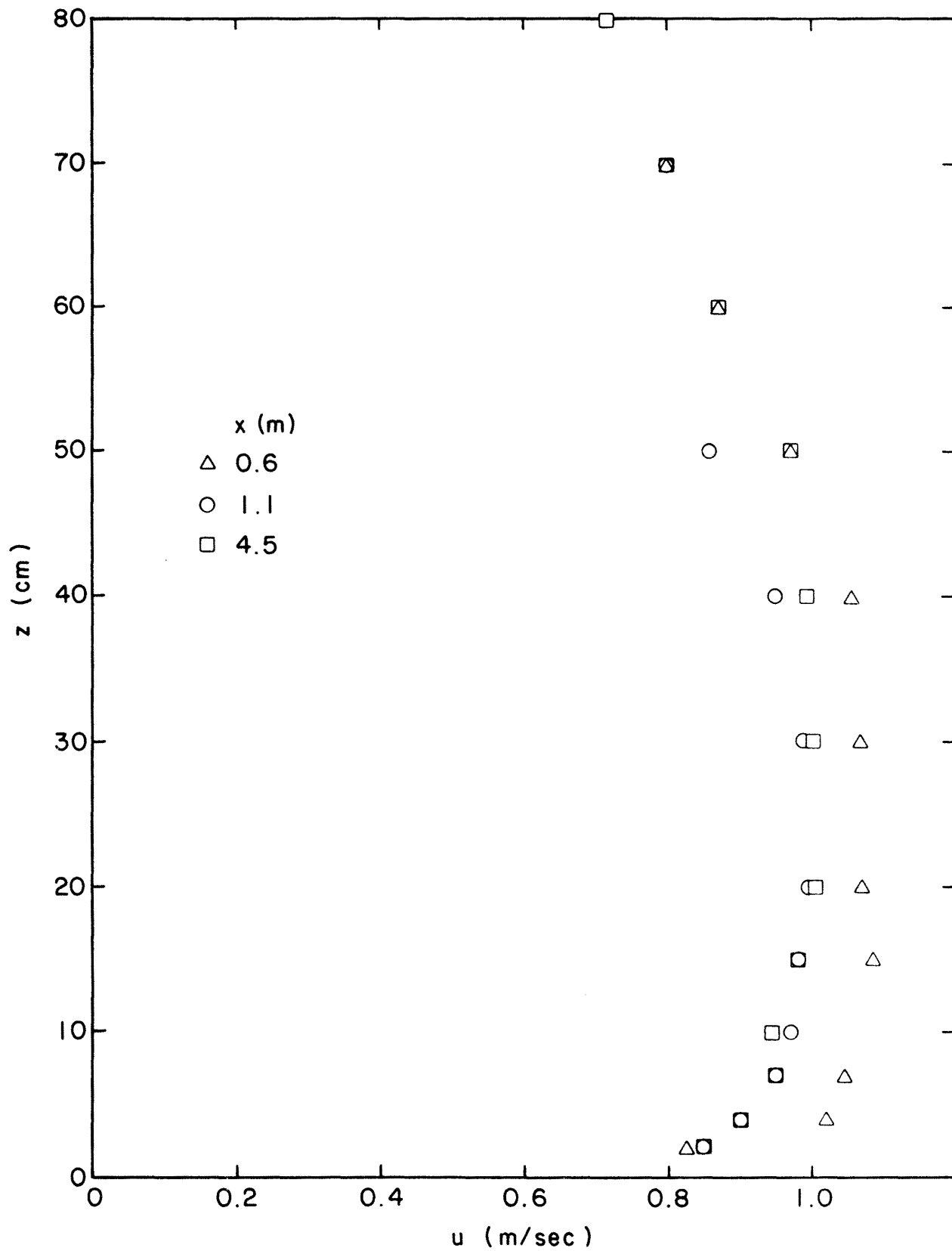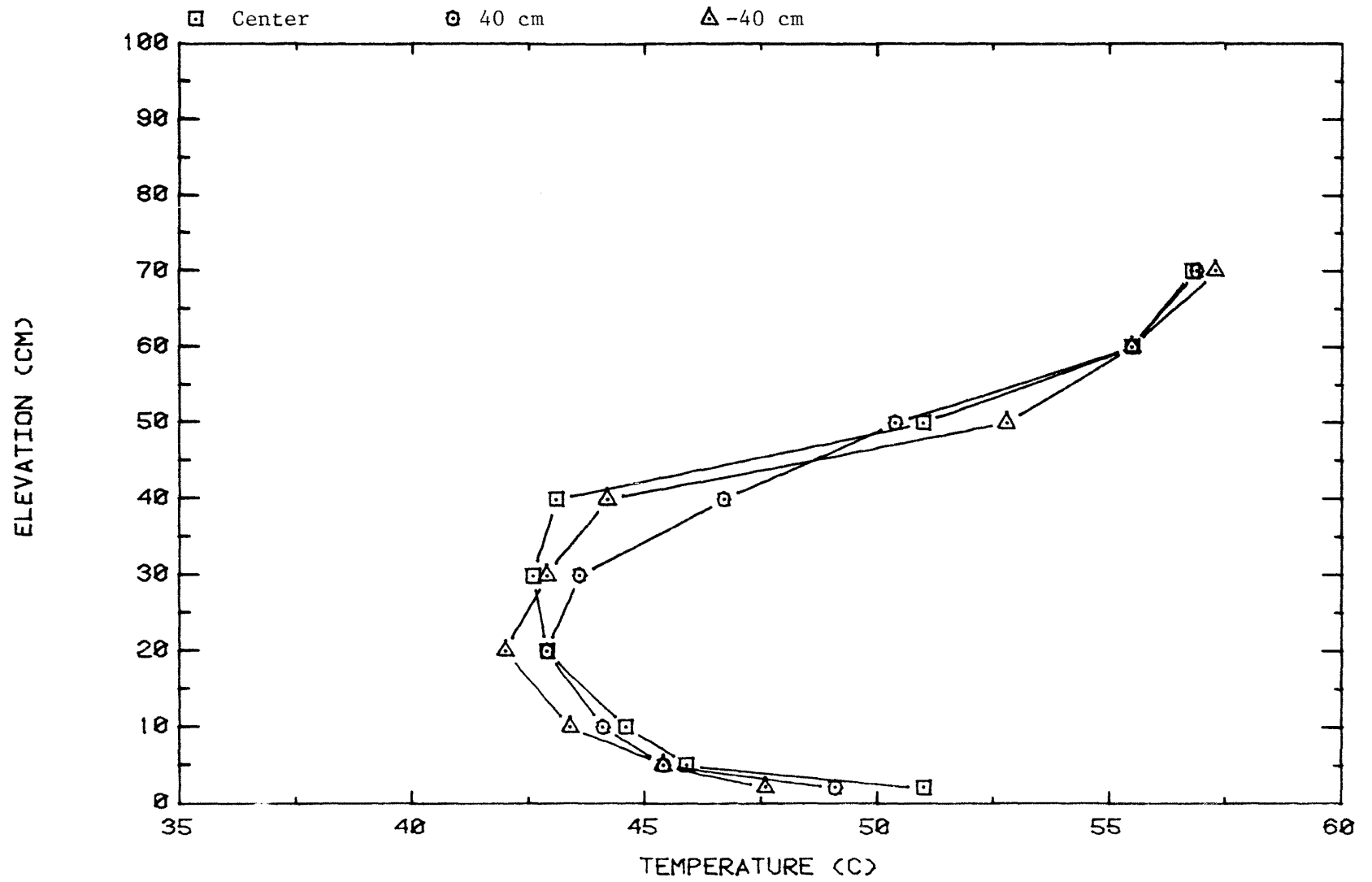
Figure 5. Mean horizontal velocity profiles.

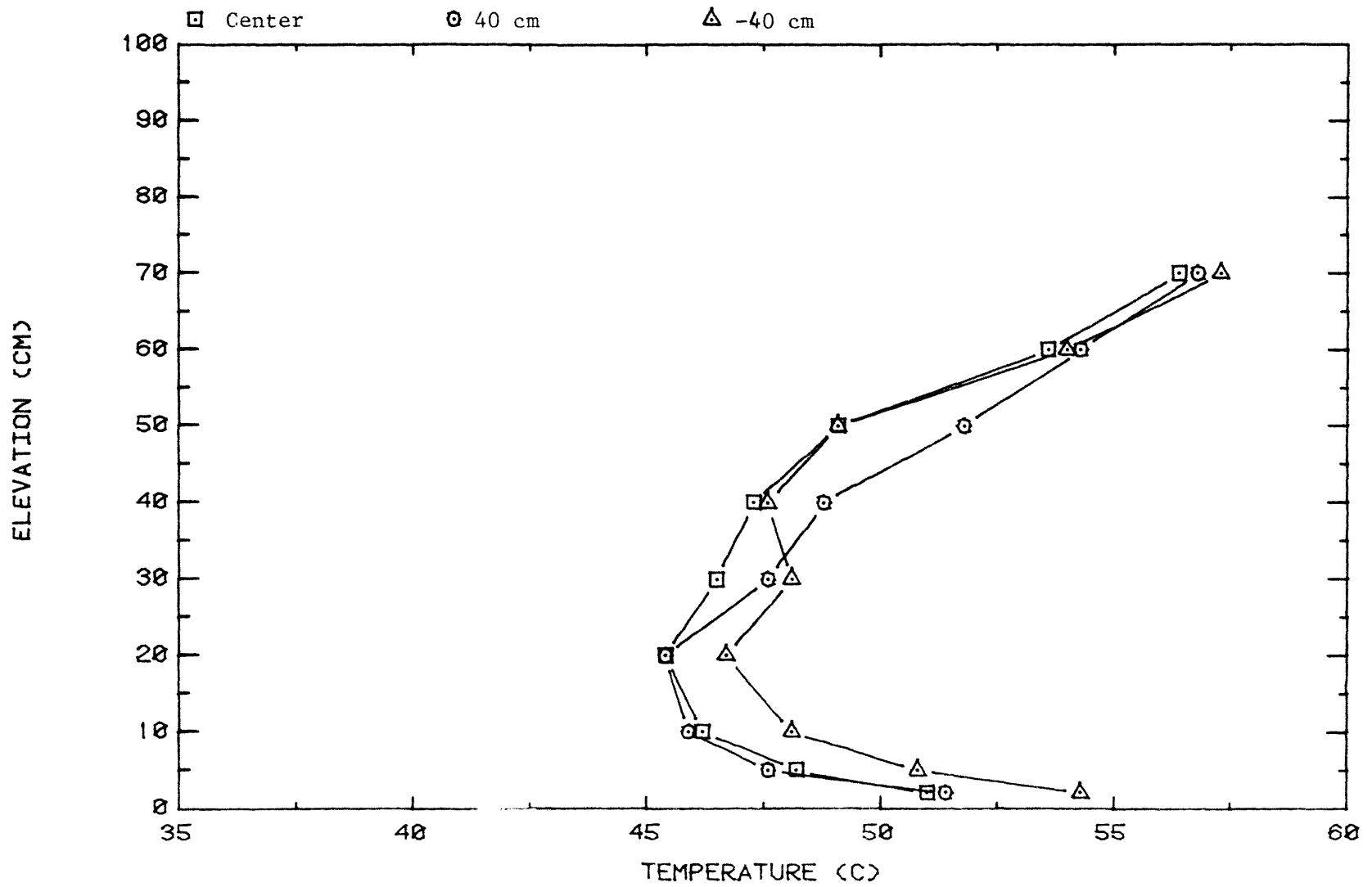Figure 6. Mean horizontal temperature profiles at x = 0.9 m; y = 0, 0.40 m and -0.40 m.

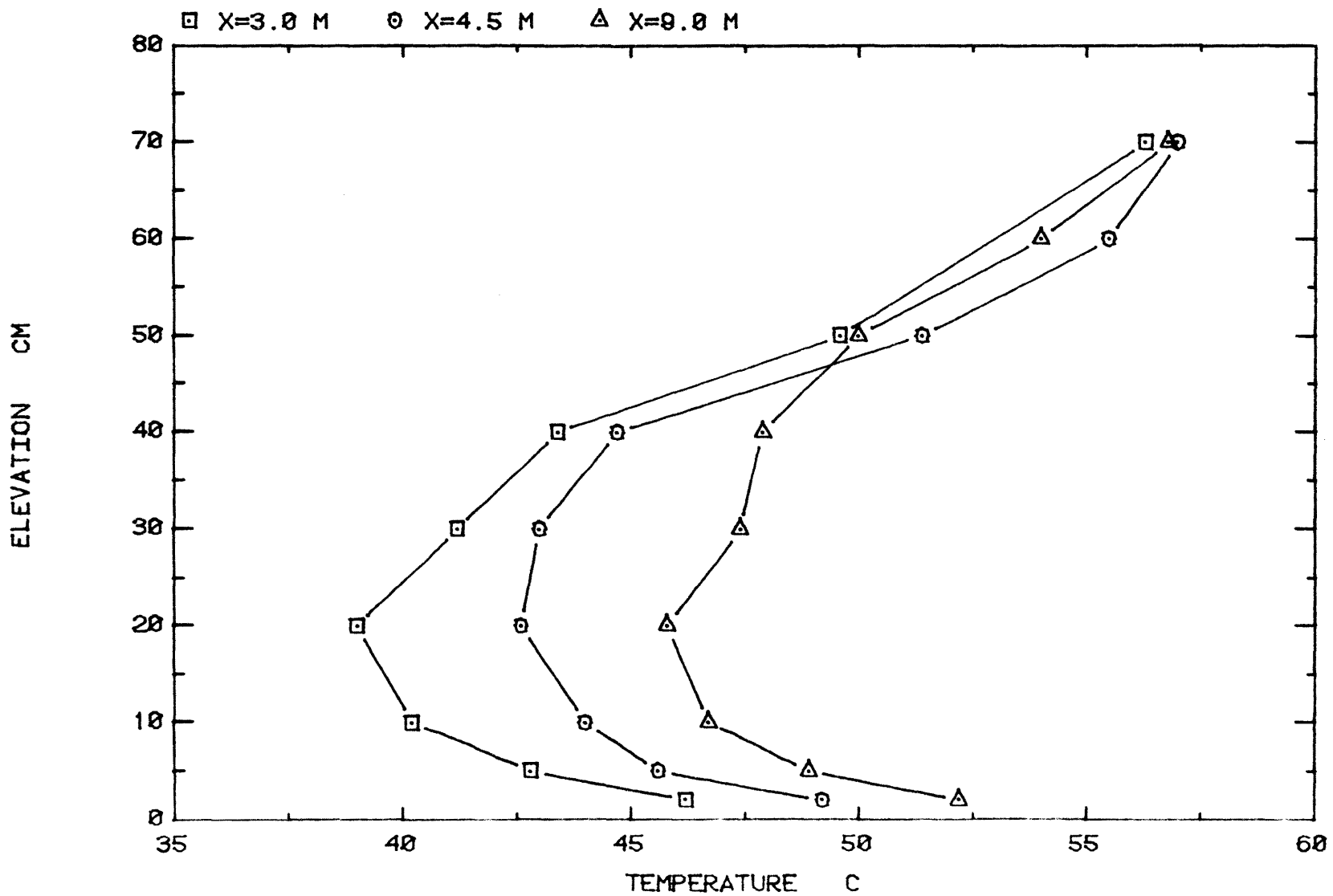Figure 7. Mean horizontal temperature profiles at x = 5.4 m; y = 0, 0.40 m and -0.40 m.

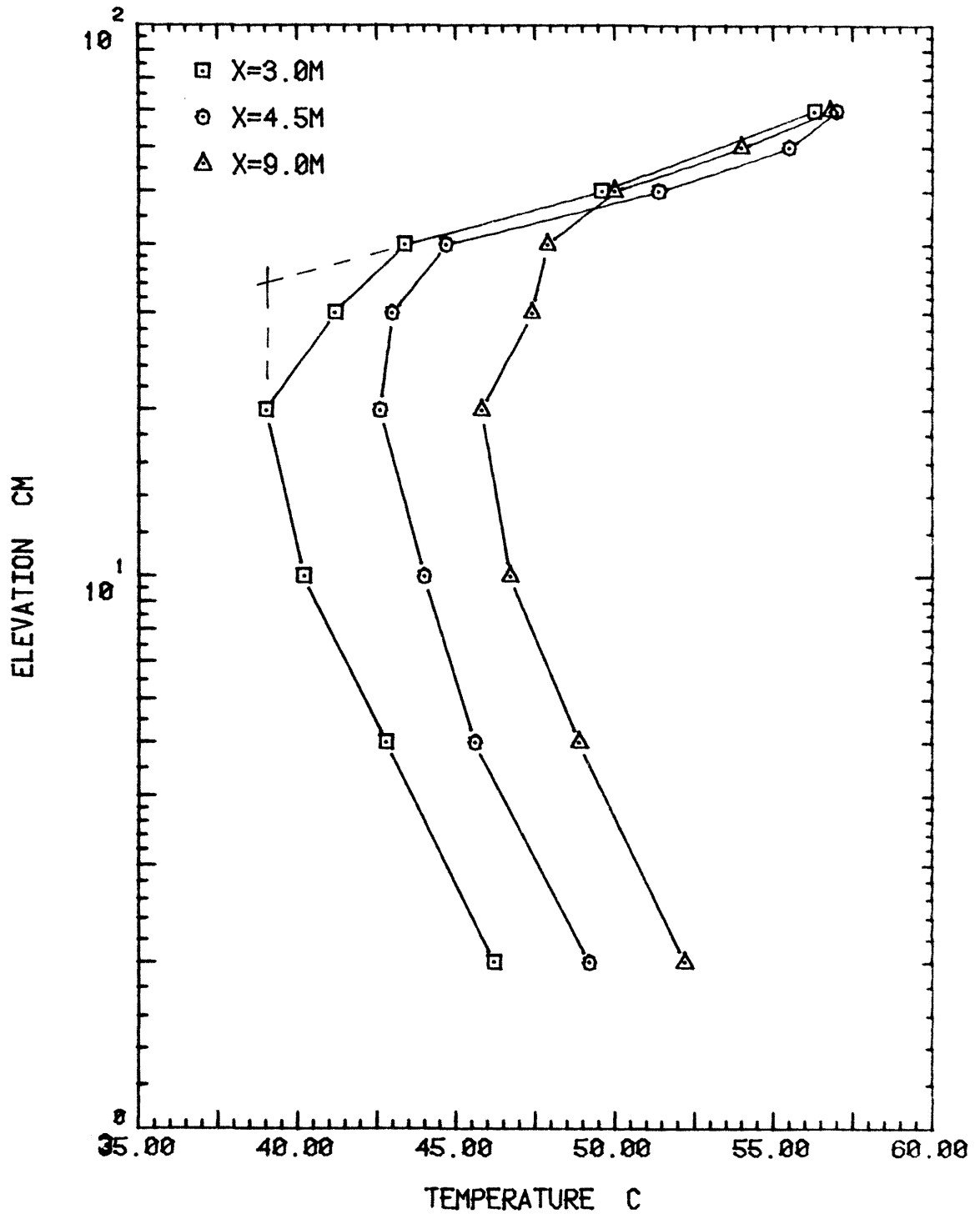Figure 8. Averaged mean horizontal temperature profiles at x = -0.6 m, 0.9 m and 5.4 m.

Figure 9. Averaged mean temperature profiles at x = -0.6 m, 0.9 m and
5.4 m, plotted in log-linear coordinates.

values of $w* = 0.16$ m/s and $T* = 2.0°C$ were obtained. The dimensionless distance $x*$, according to these values would be $x* = 0.4$ x(m).

The measurements of the temperature fluctuations σ_T^2 at $x = 0.9$ m are plotted in dimensionless form in Figure 10, which was reproduced from Caughey (1981)[4]. One sees from this figure that the measurements in the wind-tunnel simulation are consistent with the data measured in the water-tank simulation and in the atmosphere, except that the large peak at $z = h$ is missing. It is postulated that the absence of the peak might be due to the mild inversion in the wind-tunnel simulation.

The rms value of the vertical velocity fluctuation σ_w measured at $z/h = 0.4$ was estimated to be of the order of 0.07 m/s, giving a value of $\sigma_w/w* = 0.43$ and $\sigma_w^2/w*^2 = 0.19$, slightly smaller than the measurements presented in Figure 2. (It should be stressed again that the measurements of the vertical velocity fluctuations were very crude.)

The probability density distributions (PDD) of the dimensionless vertical velocity fluctuations and the temperature fluctuations, $P(w/\sigma_w)$ and $P(T/\sigma_T)$, measured at $z/h = 0.2$ and $x = 0.9$ are presented in Figure 11. The PDD is defined so that $\int_\infty^\infty P(x)dx = 1$ and, since the average values of the fluctuating quantities is zero, it is also required that $\int_\infty^\infty x\, P(x)dx = 0$.

The observed nonGaussian, positively skewed PDDs are important features of the mixed layer. They show that more than 60 percent of the time cool air is sinking down through the mixed layer toward the ground. Ascending hot air, which has much higher speeds than the sinking air, is encountered during less than 40 percent of the time, so that mass is conserved. This positive skewness of the positively correlated, vertical velocity and temperature fluctuations is indicative of the localized thermal structure with strong upwind velocities.

As the fast upward-moving air encounters the inversion base, its motion is reversed. Thus the skewness in the PDD closer to h, and close to the ground, should be smaller, as the data shown in Figure 12 for $h/D = 0.75$ confirm. The data appears to be consistent with the PDD shapes derived by Lamb (1981)[14] from the numerical simulation of Deardorff (1974)[7].

3.2 The Concentration Field

The crosswind concentration profiles measured in the study were found to be Gaussian; namely

$$C(x,z,y) = C(x,z,o) \exp[-y^2/(2\sigma_y^2)]$$

The values of σ_y, calculated from the horizontal concentration profile, for the ground-level source ($z_s/h = 0.0175$) are presented in dimensionless form in Figure 13 together with earlier data collected by Lamb (1981)[14]. As one sees, the values measured in the present wind-tunnel simulation are very close to those measured in the water-tank simulation (Deardorff and Willis, 1975)[10].
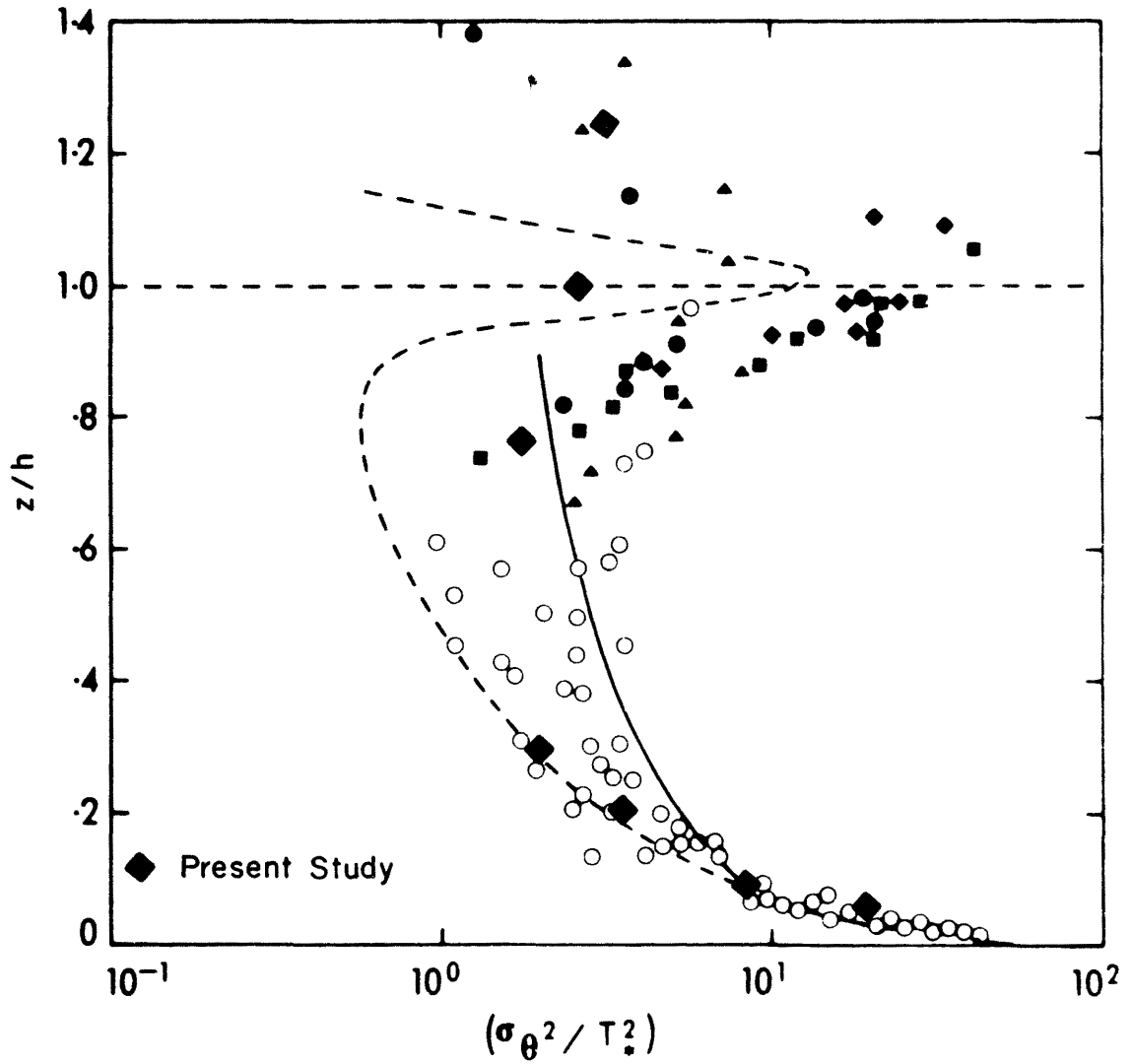
Figure 10. The normalized temperature variance. The solid line represents the free convection prediction and the dashed line the S1 case from Willis and Deardorff (1974)[17] (Caughey and Palmer, 1979)[3].
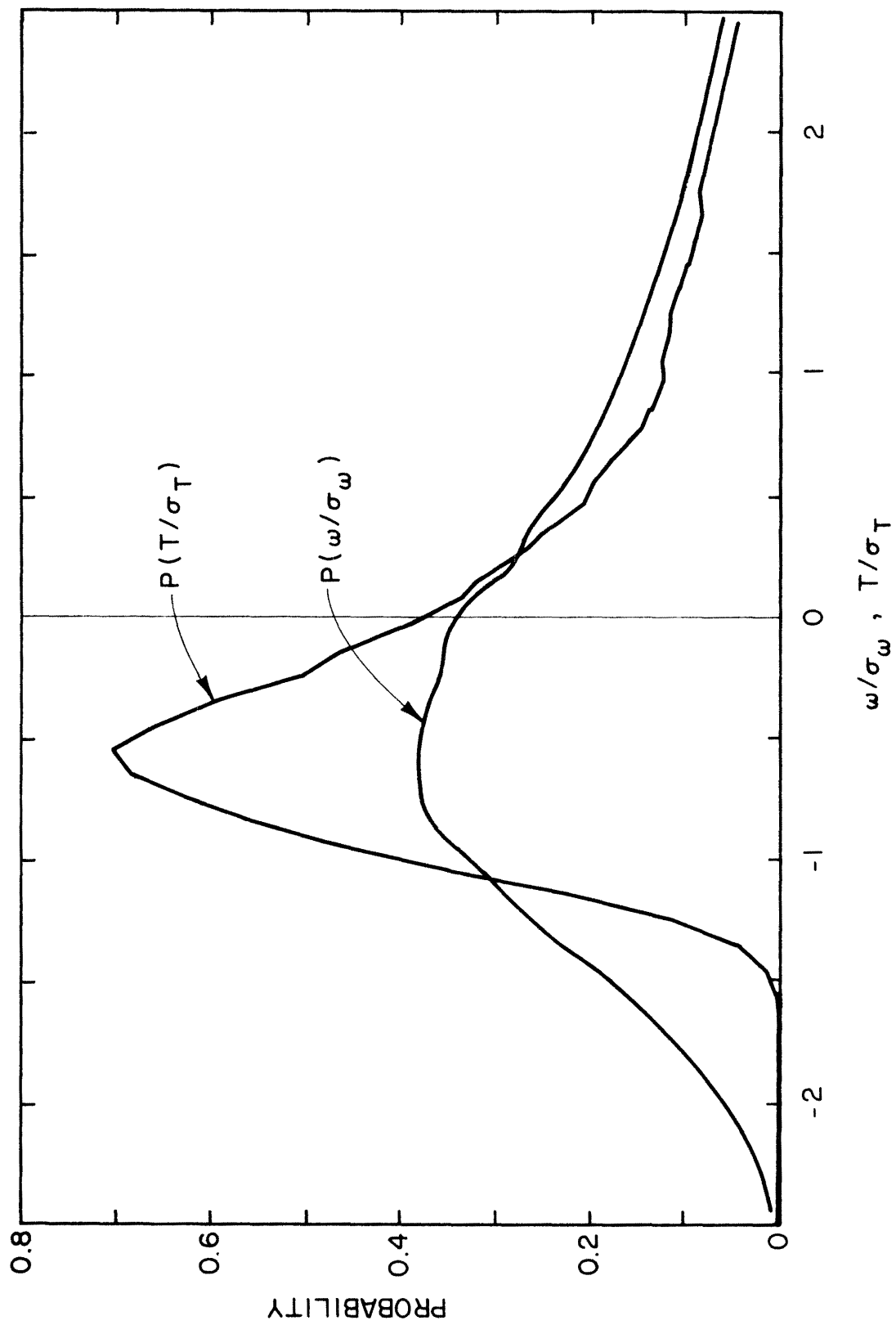
Figure 11. Probability density distributions of the normalized temperature and vertical velocity fluctuations at z/h = 0.
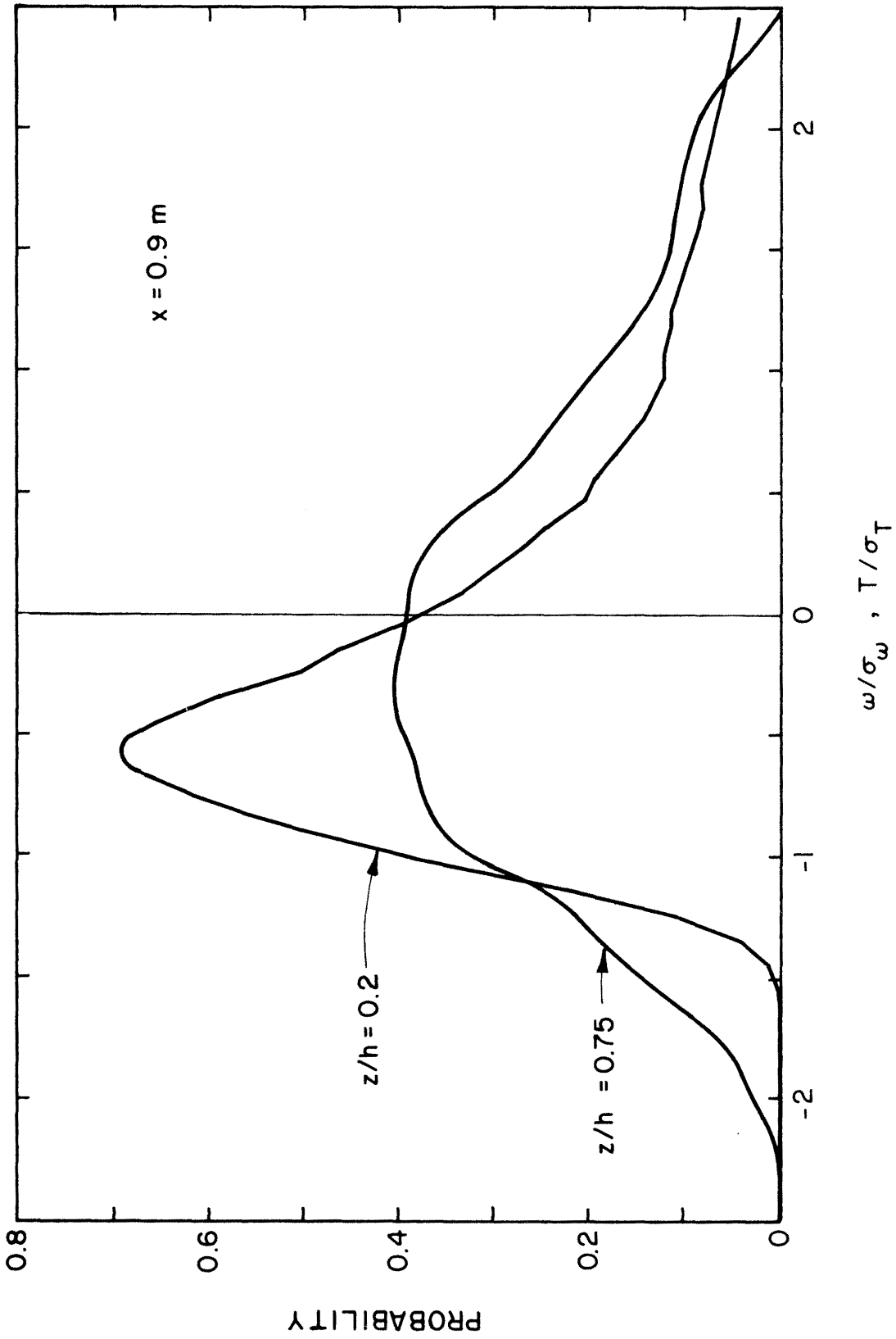
Figure 12. Probability density distributions of the normalized temperature fluctuations at z/h = 0.2 and z/h = 0.75.
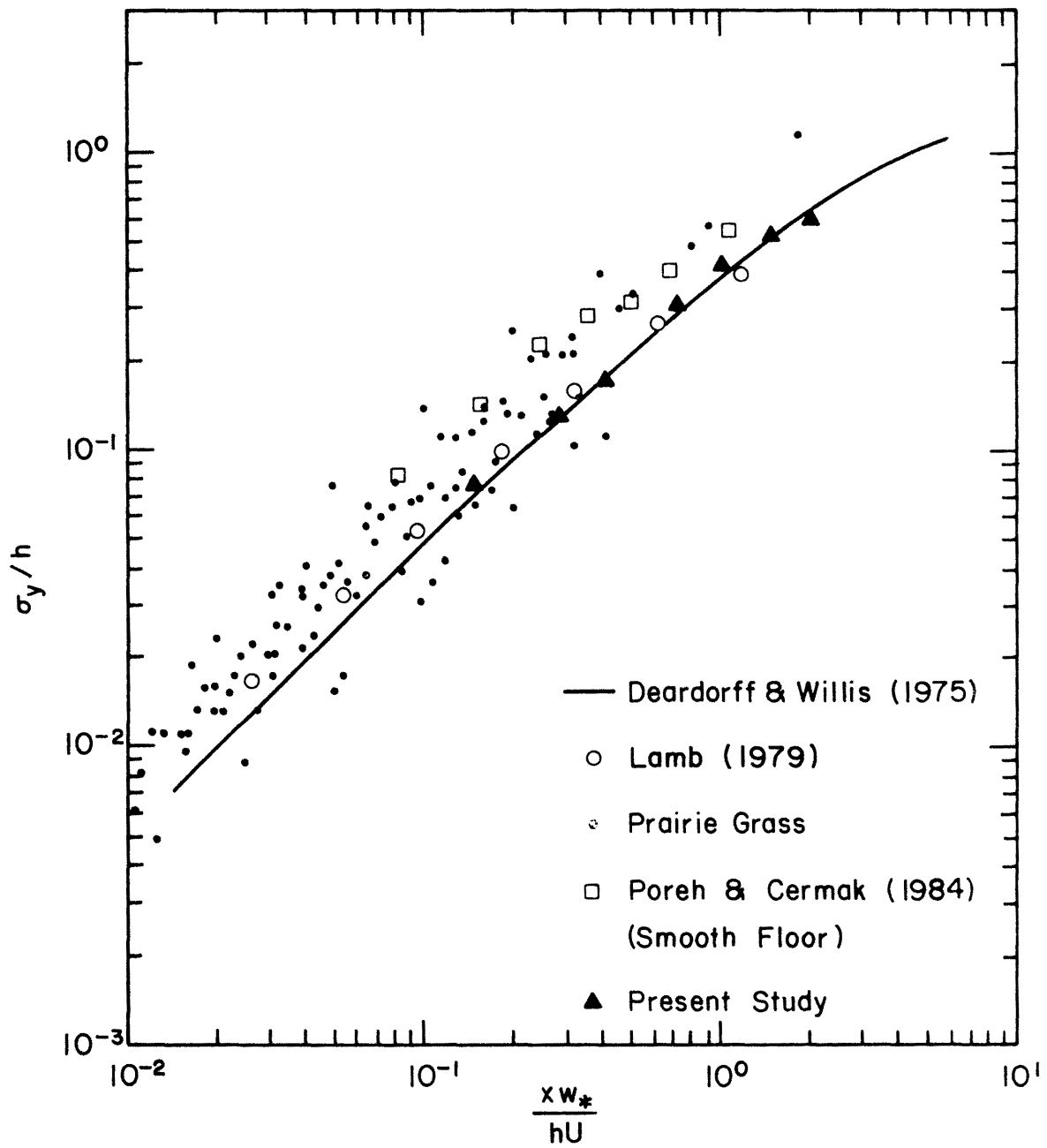
Figure 13. Dimensionless crosswind dispersion from ground-level sources.

A comparison of the crosswind spread from the ground-level source and from an elevated source ($z^s = 0.61$) is presented in Figure 14. One sees that the crosswind spread of the plume from the elevated source is smaller. This result exhibits a unique feature of diffusion in the CBL. In adiabatic boundary layers the size of the eddies increases with the distance from the ground and thus the crosswind diffusion rate increases with the height of the source. The large eddy structure of the CBL, of the order of h, dictates an increase of the lateral velocity fluctuations near the ground, where descending air reverses its direction and produces lateral and longitudinal velocities, which causes a larger lateral diffusion near the ground.

The measured average vertical diffusion of the plumes within the CBL is presented in Figures 15-17 where the dimensionless crosswind integrated concentrations

$$\frac{C^y(x,z)Uh}{Q} = \frac{Uh}{Q} \int_{\infty}^{\infty} C(x,z,y)dy = \frac{Uh\sqrt{2\Pi} \, \sigma_y C(x,y,o)}{Q}$$

are plotted versus x^* and z/h. The values of $C^y(x,z)$, were determined using the values of σ_y, which had been calculated from the lateral concentration profile at the height where $C(z,x,o)$ is maximum, assuming that σ_y is not a function of z.

Figure 15 shows the vertical diffusion of the plume from a source at $z^s/h = 0.61$. One clearly sees that the average plume descends down from the source towards the ground at a downward velocity of approximately $0.26 \, w^*$. It is noted that this value is close to the mode of the vertical velocity fluctuations within the mixing layer, see Figure 10.

From the concentration profile at $x^* = 1.48$ ($x = 3.7$ m) one sees that only 6 percent of the plume had diffused at this distance beyond the nominal height of the inversion base. Further downstream, however, the plume diffuses above that height, both because the height of the inversion base is higher than the nominal height of 40 cm and because the stable stratification of the air above the inversion base had been greatly eroded. Thus, the data for the larger values of x^*, particularly near the inversion base, is not typical for CBL capped by strong inversions and it should be evaluated taking this particular situation into consideration.

The average diffusion from the ground-level source is presented in Figure 16. The initial diffusion pattern is similar to that of plumes in shear dominated boundary layers. After $x^* = O(0.5)$, however, the position of the maximum vertical concentration climbed up at an angle of approximately $0.7 \, w^*/U$. Unfortunately, at $x^* > 1.5$ the ascending plume penetrated the weak inversion and a clear deflection from the nominal inversion base, which is expected for strong inversions, not observed in the data.
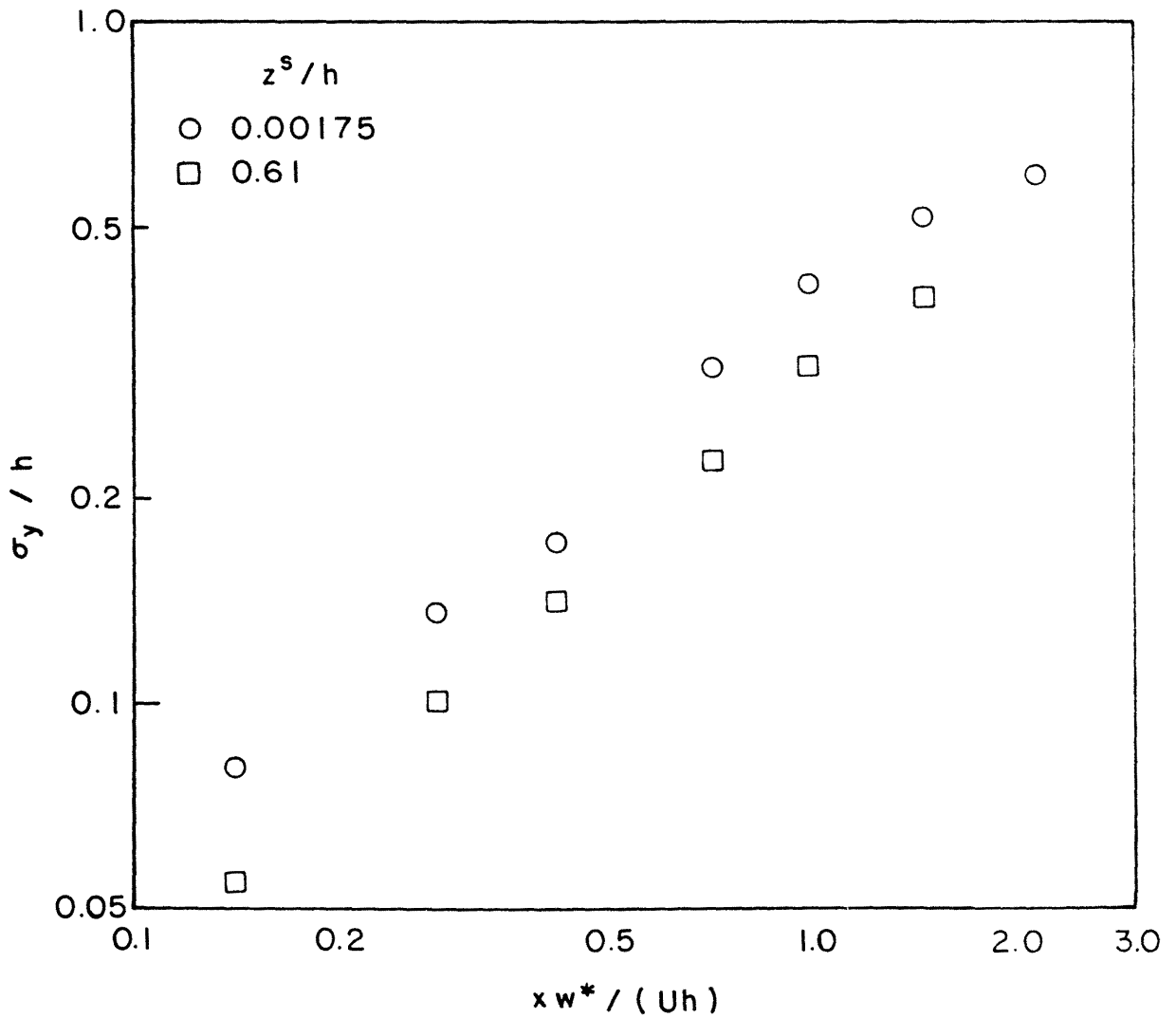
26

Figure 14. Measured dimensionless crosswind dispersion of plumes from sources at different heights.
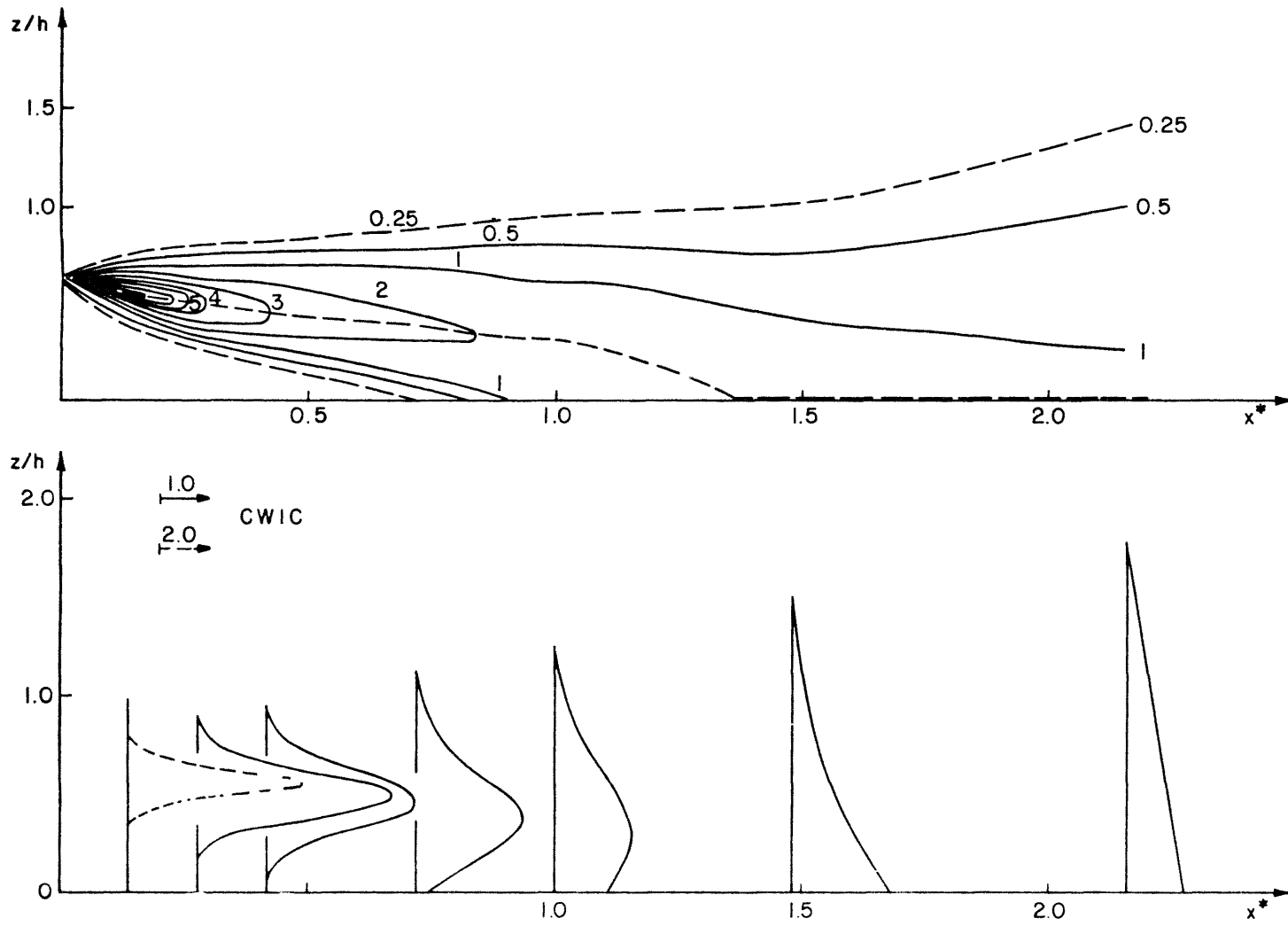
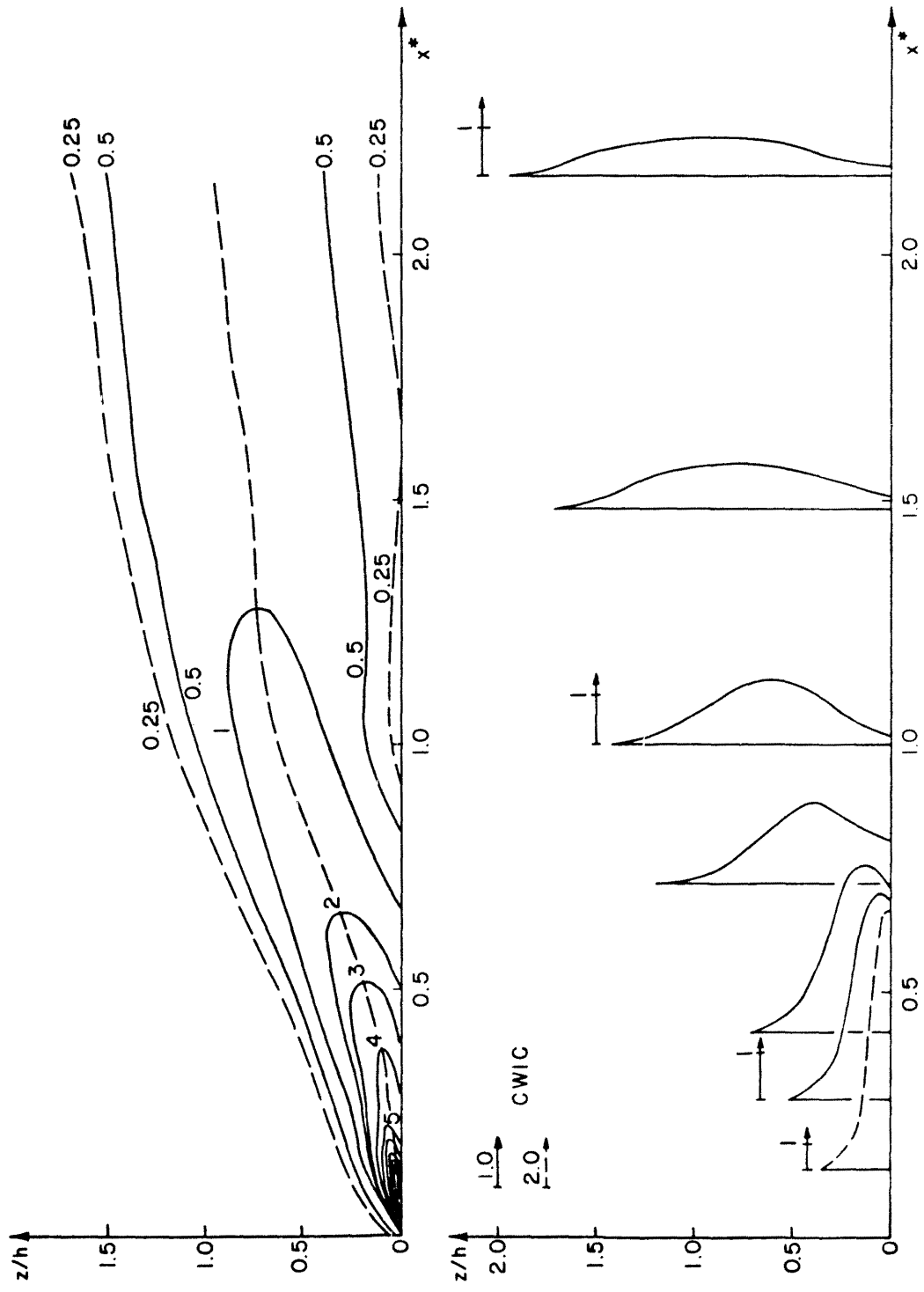Figure 15. Measured dimensionless crosswind integrated mean concentrations for $z^s/h = 0.61$.

Figure 16. Measured dimensionless crosswind integrated mean concentrations for $z^s/h = 0.6175$.
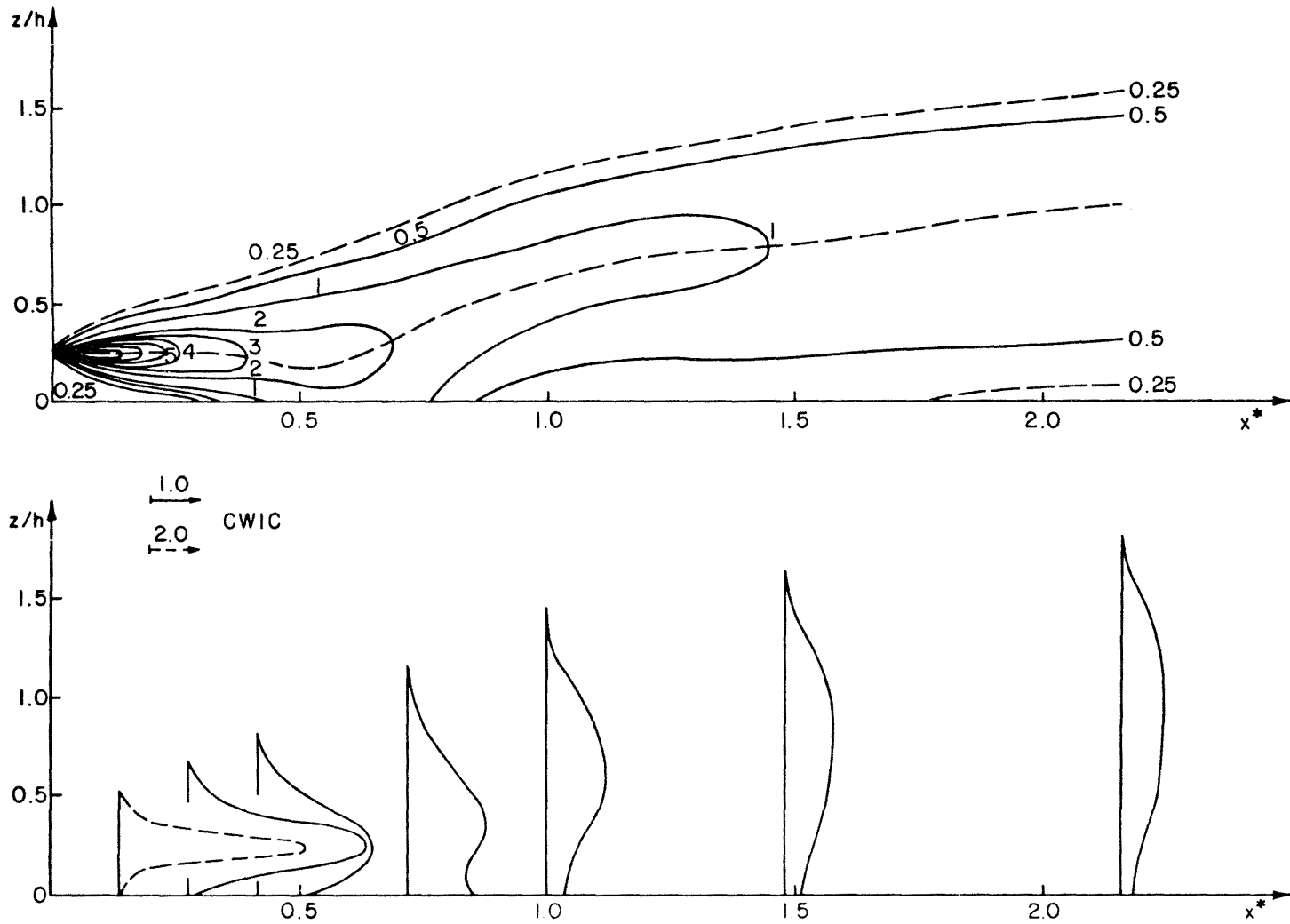
Figure 17. Measured dimensionless crosswind integrated mean concentrations for $z^S/h = 0.25$.

The average plume from the source at $z^S/h = 0.25$ is shown in Figure 17. One sees an initial descent towards the ground, followed by a subsequent rise towards the inversion base.

The measured ground-level maximum concentrations of the three plumes are shown in Figure 18. The calculated crosswind integrated concentrations at ground level for the three plumes are shown in Figure 19. The figures demonstrate that at certain distances from the source, of the order of $x^* = 1$, higher ground-level concentrations are obtained from elevated sources rather than from ground-level sources. The measured cross wind integrated concentrations at $z = 0$ for the ground-level source are compared in Figure 20 with other data collected by Lamb (1981)[14]. The wind-tunnel simulation appears to be consistent with the rest of the data. The values measured around $x^* = 1$ are smaller than those measured in the water-tank simulation, partially due to the weak inversion at this region, but they seem to be close to those measured in the Prairie Grass experiment.

In Figure 22 we have plotted the ground-level, crosswind-integrated concentrations for the sources at $z/h = 0.0175$ and 0.25 on the figure presented by Briggs (1984a)[1], which includes the BAO measurements of ground-level concentrations due to both ground-level sources and elevated sources.

Our measurements around $x^* = 1$ appear to be slightly lower than the BAO data for the ground release. It should be noted, however, that the BAO concentration data were measured above the ground at $z = 75$ m.

In Figure 23, reproduced from Briggs (1984a)[1], the measured cross wind integrated concentrations are presented in a coordinate system based on z^S rather than h. Such a presentation is useful for calculating the maximum ground-level concentration by sources at different heights. It shows that the peak values of the measured integrated cross wind ground-level concentrations is of the same order of magnitude as that of the peaks in previous studies: $C^y U z^S/Q = O(1)$, and that the peak occurs around $x w^*/(z_s U) = 2$. The region of increased ground-level concentration in the present study is, however, much smaller.
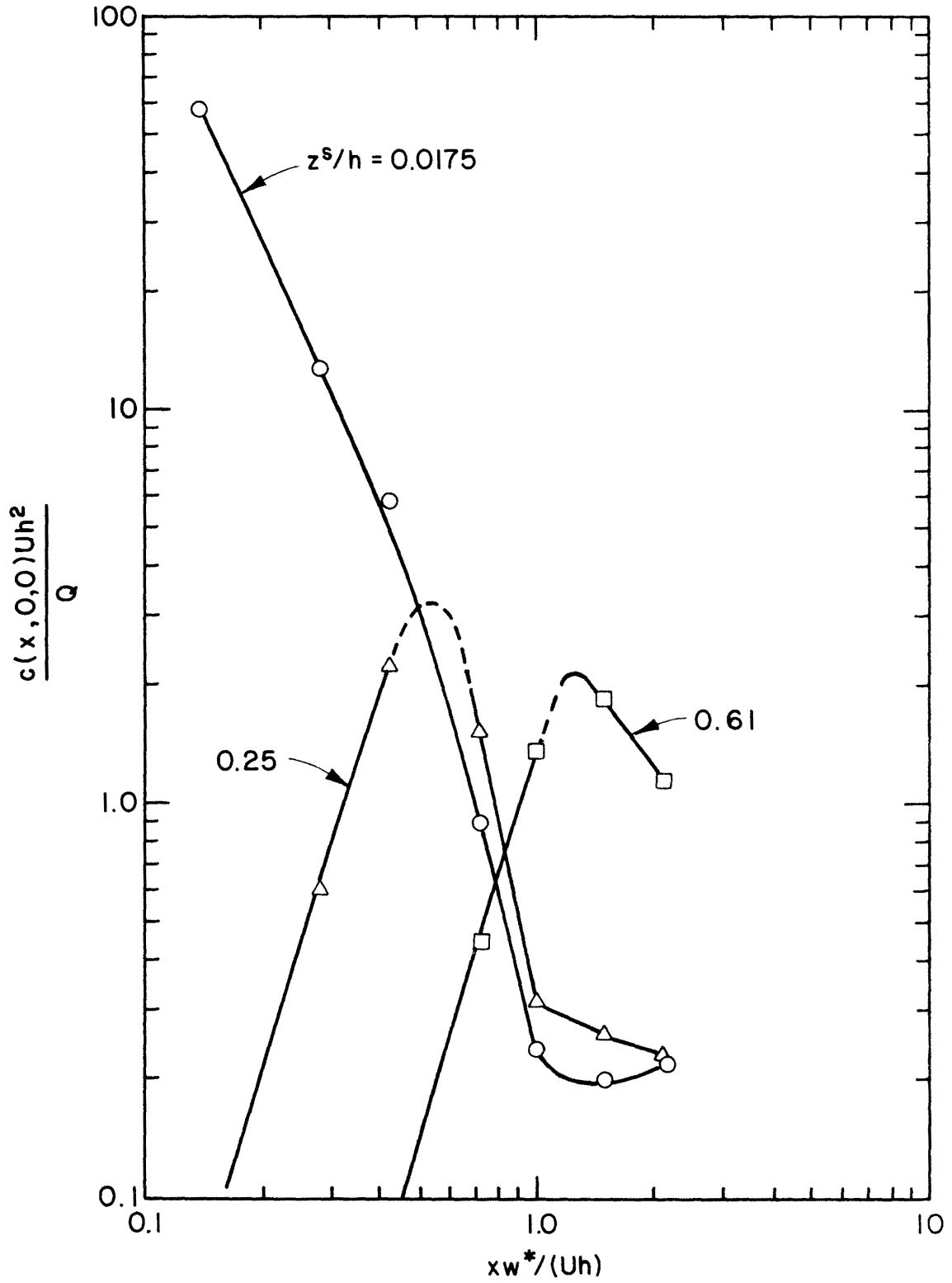
Figure 18. Measured dimensionless ground-level concentrations for sources at different heights.
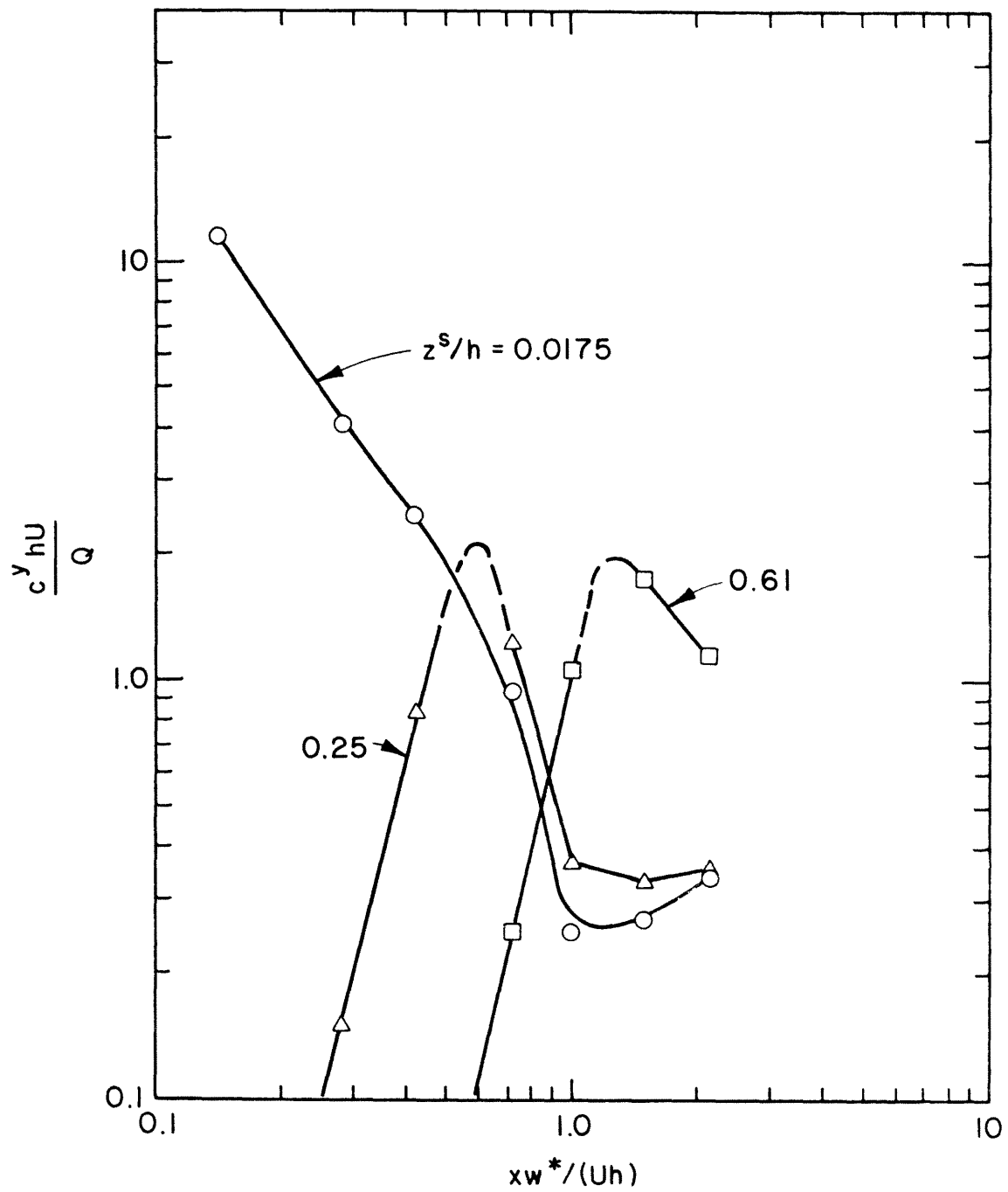
Figure 19. Measured dimensionless crosswind integrated ground-level
concentrations for sources at different heights.

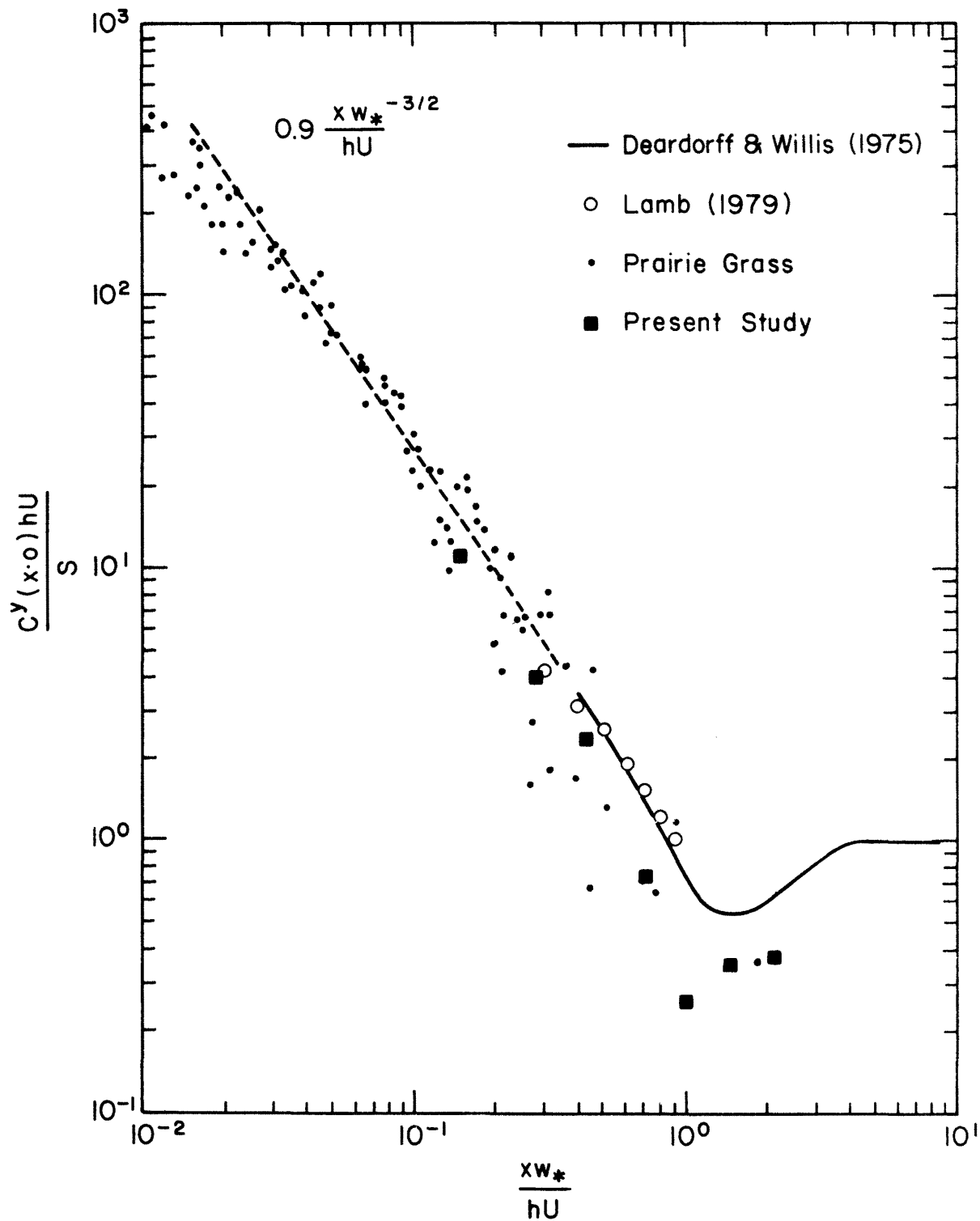Figure 20. Crosswind integrated ground-level concentrations from ground-level sources (original figure from Lamb, 1981)[3].
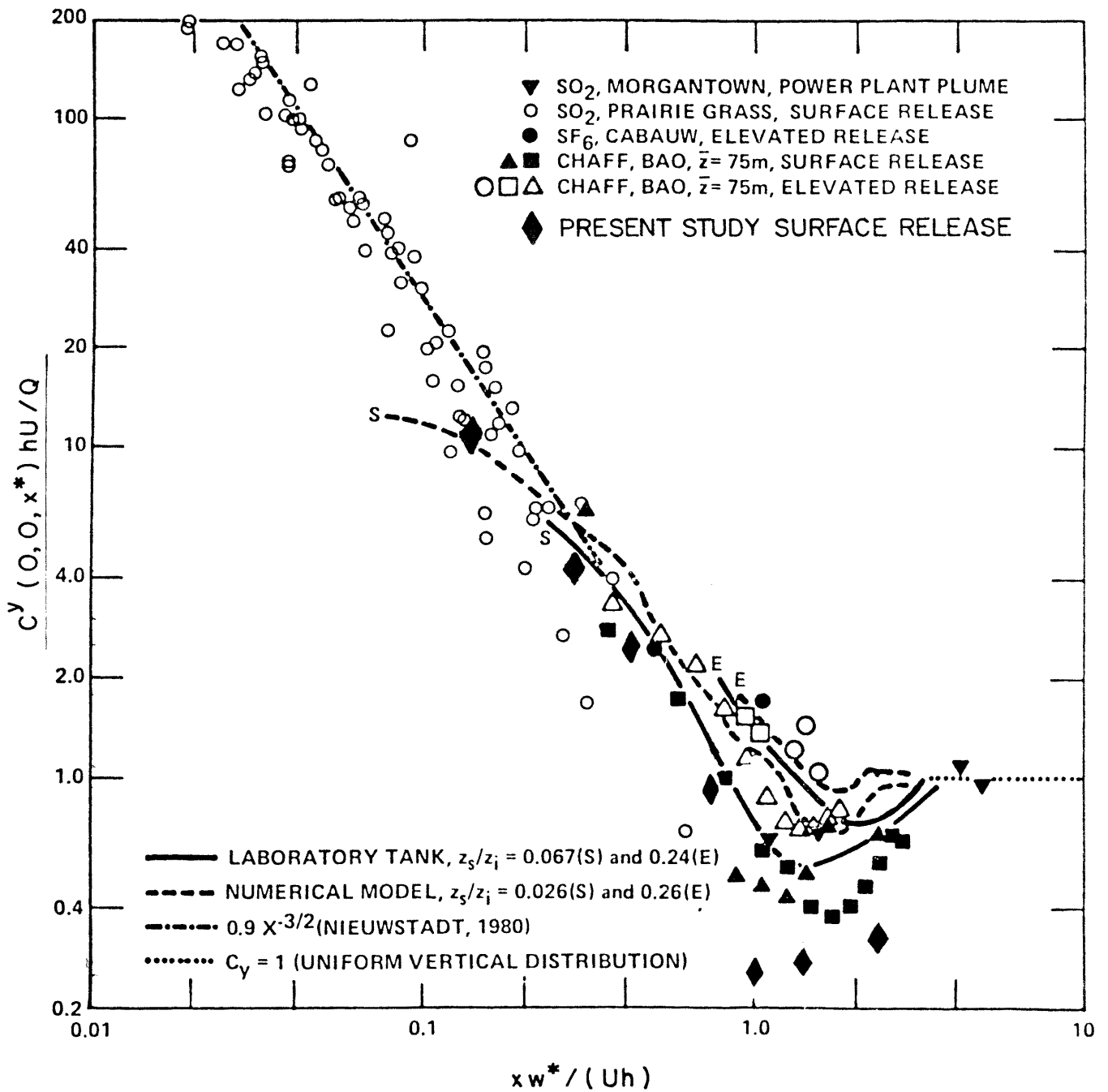
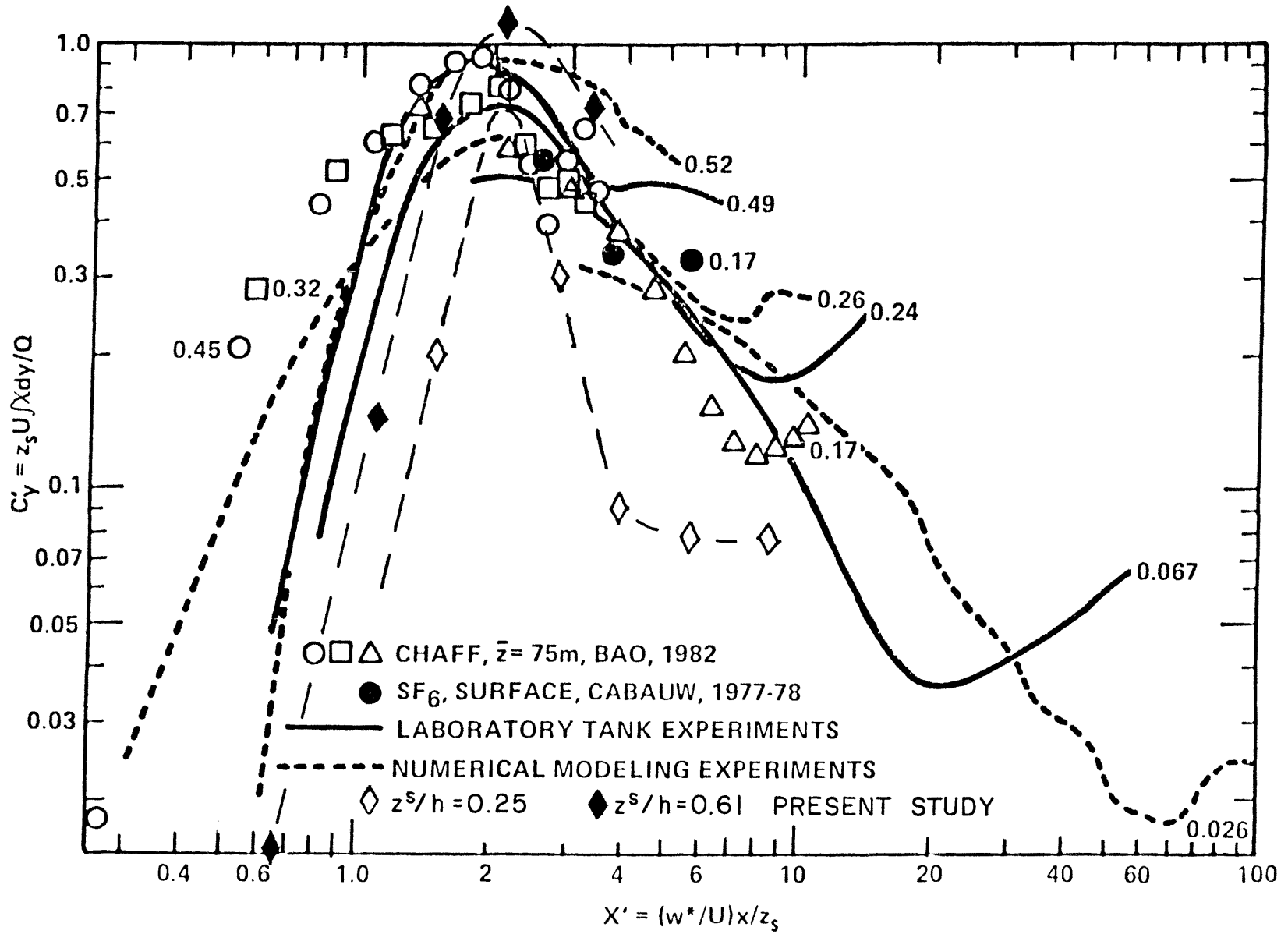Figure 21. Crosswind integrated ground-level concentrations (original figure from Briggs, 1984a)[1].

Figure 22. Crosswind integrated concentration near the surface nondimensionalized with z_s, U and Q versus $(w^*/U)x/z_s$ (original figure from Briggs, 1984a)[1].

4   DISCUSSION AND CONCLUSIONS

Convective boundary layers (CBL) are frequently encountered over both land and oceans, during periods of weak winds and upward flux of heat. It has long ago been recognized that the widely used Gaussian model fails to describe with sufficient accuracy the unique nature of diffusion in such boundary layers, but only in the last decade a better description of this particular case has emerged. The reader is referred to the outstanding monograph of Lamb (1981)[14] for a detailed discussion of the subject.

The unique, and in many ways surprising, nature of diffusion in CBL is manifested by comparison of Figures 15 and 16, which give the mean cross-wind-integrated-concentration fields for plumes from an elevated source and from a ground level source. The plume from the elevated source appears to descend rapidly down, whereas the plume from the ground level source appears to rise from the ground at $x^* = 0(0.5)$ so that the "trajectories" of the two plumes seem to intersect. Such a result is contrary to our experience with diffusion in shear flows and is usually not visible in nature. It is not surprising, therefore, that some doubts were initially raised as to whether the water tank experiments of Willis and Deardorff (1974,1976)[17,18], in which the phenomenon was first observed and which did not have any mean velocity and shear, correctly describe atmospheric convective boundary layers.

It now appears that the available field data, the results of numerical models, as well as the results from the present and the earlier wind-tunnel simulations (Poreh and Cermak, 1984)[16] in which mean wind was present, provide sufficient support for the validity of the basic formulation of diffusion in CBL in terms of the characteristic velocity w^* and the height of the layer, as proposed by Deardorff and Willis (1975)[10].

Wind-tunnel simulation are particularly advantageous in studying cases where both the convective velocity and the shear velocity have significant effect on diffusion, namely h/L < 10 and in the surface layer, z/L < 1.

To interpret correctly the meaning of Figures 15 and 16 and the reasons for the above discussed results one should take into consideration the turbulence structure of the CBL, which is dominated by strong thermals. The upward speed of the thermals is of the order of w^*. To compensate for this upward flux of mass, downdrafts of air, with velocities of the order of $0.4\ w^*$ are created over large areas. This structure has manifested itself in the skewed probability density distribution functions of both the vertical velocity fluctuations and the temperature flucuations, shown in Figure 11. Another important feature of CBL is the very large time scale of the eddy motion. Since the large, and energy containing eddies are of the order of h, the time scale of motion is larger than $1.5\ h/w^*$. Thus, the mean concentration fields plotted in Figures 15-17 do not resemble at all visible plume trajectories as they give mean concentrations obtained over times much larger than h/w^*, of the order of one hour or more in the atmosphere.

The observed downwards motion of the mean plume from the elevated source is due to the fact that most of the time the plume encounters sinking air. It must be realized, however, that for about forty percent of the time it also encounters ascending air and that is why its mean vertical spread is very large. Plumes from ground-level sources initially diffuse near the ground but will eventually be raised upward by thermals. This is the reason why $\sigma_z(x)$ curves for unstable flows (A and B) in the conventional Gaussian model, which are based on ground level concentration measurements, showed a sharp growth at distances above 500 m.

It has been demonstrated that wind-tunnel simulations can reproduce the basic features of diffusion in CBL and as argued earlier such simulations are particularly attractive for studying cases where the effect of the shear generated turbulence is not negligible. Wind tunnels can also be used to study the effect of topography or nonuniform heating of the ground on diffusion in CBL. It is usually assumed that the thermals and downdrafts in the CBL are randomly distributed. It is quite plausible, however, that nonuniform boundary conditions at the ground will generate upward motion in certain locations and thus produce a persistent non-homogeneous turbulent structure which could drastically effect diffusion from sources in certain locations (Briggs, 1984a)[1]. Finally, wind-tunnel simulations can be used to study the instantaneous shape of plumes in CBL.

Using the presently available wind-tunnel configuration, it was difficult to produce a CBL with a strong inversion which is much longer than $x^* = 1.5$. It is believed that this can be overcome by increasing the area of the cooling plates, shown in Figures 3 and 4, thus increasing the strength of the inversion, and slightly decreasing the value of the heat flux.

LITERATURE CITED

1. Briggs, G. A., (1984a), Diffusion modeling with convective scaling and effects of surface inhomogeneities, AMS Specialty Conference on Air Quality Modeling of the Urban Boundary Layer, Baltimore, Md.

2. Briggs, G. A., (1984b), Private communication.

3. Caughey, S. J. and S. G. Palmer, (1979), Some aspects of turbulence structure through the depth of the convective boundary layer, Quart. J. Roy. Meteor. Soc., 1905, pp. 811-827.

4. Caughey, S. J., (1981), in Niewstadt and van Dop (1982).

5. Cermak, J. E., (1981), Wind tunnel design for modelling of atmospheric boundary layer, J. of Eng. Mech. Div., ASCE 107, No. EM3, pp. 623-642.

6. Chorley, L. G., S. J. Caughey and C. J. Readings, (1975), The development of the atmospheric boundary layer: three case studies, Met. Mag., 104, pp. 349-360.

7. Deardorff, J. W., (1974), Three-dimensional numerical study of the height and mean structure of a heated planetary boundary layer, Boundary Layer Meteorolgy, 7, pp. 81-106.

8. Deardorff, J. W., (1970), Preliminary results from numerical integration of the unstable boundary layer, J. Atm. Sci., 27, pp. 1209-1211.

9. Deardorff, J. W., (1972), Numerical investigation of neutral and unstable planetary boundary layers, J. Atm. Sci., 29, pp. 91-115.

10. Deardorff, J. W. and G. E. Willis, (1975), A parameterization of diffusion into the mixed layer, J. Appl. Meteor., 14, pp. 1451-1458.

11. Izumi, Y. and S. J. Caughey, (1976), Minnesota 1973 atmospheric boundary layer experiment data report, AFGL Environmental Research Paper No. 547.

12. Lamb, R. G., (1978), A numerical simulation of dispersion from an elevated point source in the convective planetary boundary layer, Atm. Environ., 12, pp. 1297-1304.

13. Lamb, R. G., (1979), The effects of release height on material dispersion in the convective planetary boundary layer, Preprint Vol. AMS Fourth Symposium on Turbulence, Diffusion and Air Pollution, Reno, Nevada.

14. Lamb, R. G., (1981), Diffusion in the CBL, in Nieuwstadt and van Dop (1982).

15. Nieuwstadt, F. T. M. and H. van Dop, (1982), Editors, Atmospheric Turbulence and Air Pollution Modeling - A course held in The Hague, September 1981, D. Reidel Publishing Co., Boston, Massachusetts, U.S.A.

16. Poreh, M. and J. E. Cermak, (1984), Wind tunnel simulation of diffusion in a convective boundary layer. Boundary-Layer Met., 30, pp. 431-455, Presented at 29th OHOLD Biological Conference, Zichron Ya'Acov, Israel (1983).

17. Willis, G. E. and J. W. Deardorff, (1974), A laboratory model of the unstable planetary boundary layer, Jour. Atmos. Sci., 31, pp. 1297-1307.

18. Willis, G. E. and J. W. Deardorff, (1976), A laboratory model of diffusion into the convective boundary layer, Quart. J. Roy. Meteor. Soc., 102, pp. 427-445.

19. Willis, G. E. and J. W. Deardorff, (1978), A laboratory study of dispersion from an elevated source within a modeled convective planetary boundary layer, Atmos. Environ., 12, pp. 1305-1311.

20. Willis, G. E. and J. W. Deardorff, (1981), A laboratory study of dispersion from a source in the middle of the convective mixed layer, Atmospheric Envir., 15, pp. 109-117.

21. Willis, G. E. and J. W. Deardorff, (1983), On plume rise within a convective boundary layer, Atmospheric Envir., 17, No. 12, pp. 2435-2447.